NOAA Technical Memorandum ERL ARL-44

REGIONAL EFFLUENT DISPERSION CALCULATIONS CONSIDERING SPATIAL AND TEMPORAL METEOROLOGICAL VARIATIONS

G. E. Start
L. L. Wendell

Air Resources Laboratories
Idaho Falls, Idaho
May 1974

noaa NATIONAL OCEANIC AND ATMOSPHERIC ADMINISTRATION / Environmental Research Laboratories

ENVIRONMENTAL RESEARCH LABORATORIES

AIR RESOURCES LABORATORIES

IMPORTANT NOTICE

Technical Memoranda are used to insure prompt dissemination of special studies which, though of interest to the scientific community, may not be ready for formal publication. Since these papers may later be published in a modified form to include more recent information or research results, abstracting, citing, or reproducing this paper in the open literature is not encouraged. Contact the author for additional information on the subject matter discussed in this Memorandum.

NATIONAL OCEANIC AND ATMOSPHERIC ADMINISTRATION

NOAA Technical Memorandum ERL ARL-44

REGIONAL EFFLUENT DISPERSION CALCULATIONS CONSIDERING SPATIAL AND TEMPORAL METEOROLOGICAL VARIATIONS

G. E. Start
L. L. Wendell

Air Resources Laboratories
Idaho Falls, Idaho
May 1974

UNITED STATES
DEPARTMENT OF COMMERCE
Frederick B. Dent, Secretary

NATIONAL OCEANIC AND
ATMOSPHERIC ADMINISTRATION
Robert M. White, Administrator

Environmental Research
Laboratories
Wilmot N. Hess, Director

PREFACE

In accordance with the letter of agreement of August 3, 1973, with the U. S. Atomic Energy Commission, Division of Reactor Research and Development, Environmental Safety Branch, the National Oceanic and Atmospheric Administration, Air Resources Laboratories, have continued their study of atmospheric transport and diffusion in the planetary boundary layer, micrometeorology, diffusion climatology, and the application of this work to the disposal of radioactive waste gases into the atmosphere. The research is technically administered and supervised through the Air Resources Laboratories Headquarters, 8060 13th Street, Silver Spring, Md. 20910.

CONTENTS

DISCLAIMER

The Environmental Research Laboratories do not approve, recommend, or endorse any proprietary product or proprietary material mentioned in this publication. No reference shall be made to the Environmental Research Laboratories or to this publication furnished by the Environmental Research Laboratories in any advertising or sales promotion which would indicate or imply that the Environmental Research Laboratories approve, recommend, or endorse any proprietary product or proprietary material mentioned herein, or which has as its purpose an intent to cause directly or indirectly the advertised product to be used or purchased because of this Environmental Research Laboratories publication.

ABSTRACT

An objective regional trajectory analysis scheme has been combined with a Gaussian diffusion model to yield a technique called MESODIF (mesoscale diffusion). The trajectory analysis scheme utilized wind data from a network of tower-mounted wind sensors to consider the effects of spatial variabilities of horizontal wind flow near the surface, incorporated time changes in rates of diffusion, and used an upper level lid to vertical mixing. The MESODIF calculations of total integrated concentrations were compared with corresponding conventional calculations, using wind-rose joint frequency statistics (single wind station). Comparisons were made within a region about 100 by 130 km, and for time spans from 6 hr to 1 yr.

The diagnostic comparisons of regional dispersion effects from each technique showed significant differences over the range of scales considered. Effluent recirculations and stagnations, related to local wind variabilities about terrain features, were believed to produce localized zones of enhanced exposure to airborne effluents. These zones were not resolved by the conventional wind-rose model.

For short or accidental type of emissions, the greatest shortcoming of the single wind-station dispersion model was its failure to identify, when applied within a region of spatially variable winds, the subregion which would be affected.

At distances beyond about 25 to 50 km, the wind-rose model calculations were significantly biased to overestimation of annual total integrated concentrations by about an order of magnitude. The inability of the wind rose model to accommodate time changes in stability category during effluent transport to the more distant receptors was the single most influential factor of this bias.

Current usage of the wind rose technique for regional dispersion calculations, especially at the longer distances, incorporates some systematic bias in the evaluations. These shortcomings are points of concern and should be reconciled with whatever impact assessment schemes are to be utilized within the mesoscale or regional domain.

REGIONAL EFFLUENT DISPERSION CALCULATIONS CONSIDERING SPATIAL AND TEMPORAL METEOROLOGICAL VARIATIONS[1]

G. E. Start
L. L. Wendell

1. INTRODUCTION

During the last several decades, the understanding of the role of the atmosphere in dispersion of airborne material has been greatly increased. With the present body of knowledge, atmospheric dispersion calculations may be performed with confidence for distances out to several kilometers and for times of a few hours. However, calculations at greater distances, for longer times, within areas of marked topographic variability, or for atmospheric conditions which deviate from simple homogeneity, the confidence and reliability rapidly diminish. Research in recent years has begun to quantify dispersion within flows across mountain ridges, diffusion within deep canyons, and for disturbed airflows around buildings and obstacles. Likewise, significant variabilities may occur for longer time-averagings and at distances beyond a few kilometers, in light of the other significant effects noted.

From a background of several years of meteorological and climatological support of reactor siting and operations at the National Reactor Testing Station (NRTS), it was apparent that significant horizontal variability occurred in low altitude winds over the Upper Snake River Plain in southeastern Idaho. From simple meteorological considerations and later field measurement

---

[1]Research was carried out under the joint sponsorship of the Atomic Energy Commission, Division of Reactor Research and Development.

programs at other localities, these variabilities were judged to be common to many geographical settings and, therefore, were relevant to environmental-impact assessment calculations for a large number of potential sites. With these problems in mind, deployment of a network of tower-mounted wind sensors was begun in early 1968. As a consequence of data collected from this network, an initial understanding of mesoscale variability of winds has been gained. The initial results of this program have been reported by Wendell (1970, 1972).

The implications of such wind variabilities for calculations of atmospheric dispersion were recognized in 1966, and some simple diffusion model adaptations were examined (Start and Markee, 1967; Dickson et al., 1967). During the course of these examinations, it became apparent that effluent plume geometries could often attain complex forms or undergo transformations from one form into another; simple concepts such as a cross-wind-oriented line source and a continuous point source could not suitably describe these forms or remain applicable following their transformations.

Because dispersion estimates were to be made out to radial distances of 150 km and for time periods as long as a year, several current practices were suspected to be inappropriate. One such practice was the use of wind data measured at a single point. Their utilization to describe the dispersion of airborne material at distances far from the point of measurement would require an extreme degree of horizontal homogeneity in the airflow.

A surface continuous point-source was adopted for all illustrations and comparisons. More complex source configurations could have been utilized, but they would have only clouded the results with additional details.

The simplified model utilized in this project, MESODIF (mesoscale diffusion), incorporated a two-dimensional wind field within which effluent trajectories were calculated according to measured temporal and spatial variabilities of the winds (Wendell, 1970, 1972). Current practices for long-term regional pollution impact evaluations utilize the well-known stability wind-rose (WR) technique; this technique distributes the total period-source release within radial sectors emanating from the source point. The release is distributed in proportion to the frequency of source point winds blowing into the individual sectors. The comparisons of results from these two techniques do not constitute a "validation" of one technique over the other; rather, they illustrate variabilities induced by spatial and temporal changes of the winds. The research described herein was an investigation of these variabilities of total integrated concentrations within a mesoscale-sized region.

Several obvious questions come to mind when beginning an investigation of this type. First of all, will any significant differences occur between the two cited techniques? If so, will there be spatial and/or temporal boundaries on the significant differences; for example, will the two methods differ only at distances greater than 15 km, 30 km, or so forth? Will differences begin to appear almost immediately in time, but quickly disappear as soon as the point wind statistics accumulate a suitable number of occurrences in each wind category? If differences occur and either average out with longer term accumulations or remain with some residue, can physically meaningful causes or sources of these variations be identified?

A number of methods for examining these questions come to mind. Perhaps the simplest approach would be a comparison of the area frequency

distributions determined by each of the transporting wind assumptions or models (this amounts to assuming no diffusion of plume effluent and to counting the number of "exposures" resulting strictly from wind transporting of material to given receptors). This receptor-transport climatology study has been undertaken and initial results reported (Van der Hoven, 1971). Gifford (1973) aptly pointed out that these receptor climatologies should likely represent maximum differences because real plumes would have a larger size and, therefore, are more likely to smear out or to diminish any differences resulting solely from transporting winds. However, because receptor-transport climatology studies showed areas of differences as large as an order of magnitude for an annual cycle, similar diffusion-model calculations were needed to determine whether the addition of plume diffusion would negate these differences.

2. THEORY OF DIFFUSION MODELS

A continuous point source (CPS) has been postulated to examine the effects of spatial and temporal variations of the low-altitude wind flows upon time-integrated concentration estimates. Because the transporting wind flows could be expected to be curving, recirculating, and at times stagnating flows, a Gaussian simple CPS type of equation could not be used (because the plume geometry would likely be altered to the point of inapplicability). Because the CPS equation is an integration of the more general Gaussian instantaneous point-source (IPS), this IPS equation (Slade, 1968) will be the beginning point. For a ground-level source and receptors with total reflection at the earth's surface,

$$\chi(x,y,o) = \frac{2Q}{(2\pi)^{3/2}\sigma_x\sigma_y\sigma_z} \exp\left[-1/2\left[\frac{(x-\bar{u}t)^2}{\sigma_x^2} + \frac{y^2}{\sigma_y^2}\right]\right] \quad (1)$$

where

$\chi(x,y,o)$ = concentration (units/m^3),

Q = source strength (units),

x,y = distance downwind and crosswind from point of origin, respectively (m),

$\bar{u}$ = mean windspeed (m/s^{-1}),

t = time of travel of the cloud (s), and

$\sigma_x,\sigma_y,\sigma_z$ = standard deviations of effluent concentration in the downwind, crosswind, and vertical directions, respectively (m).

The σ-values used in MESODIF are the Pasquill A through F types of values (Yanskey et al., 1966) which were derived from continuous plume releases of 1/2- to 1-hr duration. The application of these rates to puff diffusion would tend to overestimate the dilution (and to underestimate the concentration) of puffs within the first few kilometers (Slade, 1968). It should be noted that the specifications of σ-values versus stability categories and trajectory distances primarily apply to distances of a few kilometers. Extrapolation of these curves to regional scale distances is substantiated by little or no data. However, because one dispersion method is to be compared to another, these factors should compensate one another because each model uses the same extrapolated curves.

If horizontal Gaussian symmetry is adopted, equation (1) may be restated as

$$\chi(x,y) = \frac{2Q}{(2\pi)^{3/2}\,\sigma_H^{\,2}\,\sigma_z}\exp\left[-1/2\left[\frac{r^2}{\sigma_H^{\,2}}\right]\right] \qquad (2)$$

where

$$r^2 = (x - \bar{u}t)^2 + y^2$$

and

$$\sigma_H = \sigma_x = \sigma_y \ .$$

Because the application of equation (2) must satisfy conditions of simple, straight-line flow and provide total integrated concentrations (TIC), equation (2) needs to be adapted. Normally, TIC values are obtained by using an integrated (with respect to the x or flow axis) form of the equation. Integration would negate the breaking of the continuous plume into appropriate subelements. Instead, what is used is an approximation to the integral by a summation of weighted concentrations of the form

$$\frac{1}{\bar{u}}\int_{-\infty}^{\infty}(\chi_{IPS})dx \quad \sum_{j=1}^{N}(\chi_{IPS}{}^{*}\delta t)_j \simeq \chi_{CPS} \qquad (3)$$

where

$x = \bar{u}{*}t$ and $dx = \bar{u}{*}dt$ are used for a transformation of variable. The summation process is similar to approximate integration by the trapezoidal rule, except the concentration at the end of a time interval j (χ_j) is assumed to prevail over the entire time interval (δt_j). The area under the Gaussian-like curve of concentration versus time is proportional to the TIC at the receptor point. Depending upon the number of intervals (plume segments) used, the approximation may converge to the integral at any desired level of accuracy.

In application, the MESODIF model disperses plume effluent through the advective transport of plume segment (puff) centers and through the diffusion of effluent puffs about their individual centers. The transport of puffs is determined from a horizontal field of spatially and temporally varying winds. The diffusion of effluents is described by distance-dependent values of σ_H (or σ_y) and σ_z (Yanskey et al., 1966). These values are specified according to a general form

$$\sigma = \sigma_o + \Delta\sigma \tag{4}$$

where

σ_o = previous value (ideally zero at the point source),

$\Delta\sigma$ = incremental change during the advective displacement just completed, and

σ = updated value following the completed advective step.

The advective related growth $\Delta\sigma$ is different for σ_y and σ_z and has various constraints to conform better to observed plume behaviors. For horizontal diffusion, σ_y is represented by the general forms (Slade, 1968),

$$\sigma_y = A*x^{.85} \quad (\text{for } x < 20 \text{ km}) \tag{5a}$$

and

$$\sigma_y = A'*x^{.5} \quad (\text{for } x \geq 20 \text{ km}) \tag{5b}$$

where

x = distance along puff trajectory from the source,

A = stability-category dependent coefficient of proportionality chosen to fit empirical curves of σ_y versus distance (Yanskey et al., 1966)

A' = stability-category dependent coefficient of proportionality for continuity at 20 km between equations (5a) and (5b).

The exponents of x in equations (5a) and (5b) were selected to fit the

σ_y-curves reported by Yanskey et al., (1966). At and beyond 20 km, the horizontal diffusion rate is slowed to the Fickian rate (proportional to the square root of time or distance). To describe σ_y during changes of stability category,

$$\Delta\sigma_y = \frac{\partial\sigma_y}{\partial x}\Delta x \qquad (6)$$

where

Δx = advective displacement or distance

and

$\frac{\partial\sigma_y}{\partial x}$ = rate of growth of σ_y derived from equation (5a) or (5b).

It should be noted that equation (6) incorporates A or A' and x through the derivatives of equation (5a) or (5b); thus the rate of growth is both dependent upon stability category and total distance traveled. Because the rate of growth is distance dependent, a value determined at the middle of the advection step just completed is the value used in equation (6).

The basic representation of σ_z is

$$\sigma_z = B^*x^\gamma \qquad (7)$$

where

B = stability-dependent coefficient of proportionality chosen to fit empirical curves of σ_z versus distance (Yanskey et al., 1966),

γ = stability-dependent exponent of travel distance, and

x = distance along puff trajectory from source.

In practice, a form like equation (4) is utilized to update the previous value, assuring that σ_z either remains constant or increases in magnitude.

For vertical dispersion, a capping stable layer or restricting lid to upward diffusion is considered (e.g., Turner, 1970). Three physical regimes are identified for specifying rates of growth of σ_z. They are: (1) a region in which the upward spreading is little affected by the presence of the capping lid, and a Gaussian distribution is assumed in the vertical; (2) a region within which thorough mixing of the entire layer has created a nearly uniform distribution of effluent between the ground and the capping lid; and (3) a region between these two in which the plume begins to be affected by the capping lid, and the vertical distribution undergoes a transition from Gaussian to one nearly uniform.

The height of the base of the capping lid or stable layer is denoted L. In MESODIF, L is specified hour-by-hour to permit an accounting for known diurnal variability of this depth of mixing. An hourly value of L is applied uniformly throughout the computational area. The effective value σ_z equals 0.8L (Turner, 1970) when the vertical distribution has approached uniformity. If previous values of σ_z already exceed 0.8L, they are held constant ($\Delta\sigma_z = 0$); they are not reduced in any manner because a negative $\Delta\sigma_z$ would imply negative diffusion. During a given hour in which an L applies, values of σ_z initially less than 0.8L are restrained from growing larger than 0.8L. Physically, this means the following. During any given hour, plume material may diffuse upward and be confined by the stable layer aloft. Material present from earlier times may have spread aloft to greater depths than permitted by the current stable layer. This earlier spreading is not compressed back into the more shallow layer now existing; it may be better visualized as being

partitioned into portions now below the stable layer and portions within or above the new stable layer. Material above the lid is dropped from further consideration.

The source emission strength Q may be specified hour-by-hour if desired. For this memorandum and the comparisons to be presented, it has been held constant at one unit per hour; each puff then contains one unit divided among the number of puffs released per hour. Removal mechanisms, such as dry deposition, precipitation scavenging, and chemical and photochemical changes, are not incorporated.

3. COMPUTATIONAL METHOD

The two essential parts of the computation are the determination of the locations of the puffs as they are carried by the wind and the calculation of the growth and subsequent dilution of each puff. A third portion of the computation involves the determination of the contribution of the puffs to the time-integrated dosage on an array of grid points. Because the model has been used for long-term releases, up to 1-yr duration, as well as for 12- to 24-hr accident simulations, significant effort has gone into making the calculations as efficient as possible without sacrificing the integrity of the result.

The portion of the model which moves the puffs is based on a simple advective process, using a time series of wind measurements from a randomly spaced array of wind stations (Wendell, 1972). The hourly averaged winds at the stations are interpolated onto a rectangular grid with a subroutine, and the movement of the puffs is computed through a time and space interpolation of the gridded wind fields. This arrangement disengages the

transport and diffusion portion of the model from the wind determination. This separation provides the option of using the model with historical or predicted winds when they are available. As mesoscale wind-prediction techniques are developed and improved or as they might vary from one region to another, these techniques will be readily usable by this model in cases where TIC predictions are required.

The periodic sampling of the puffs for summing concentrations at the grid points is based upon a distance increment rather than a specified time increment to allow a more uniform approximation to the continuous plume at both high and low windspeeds. The displacement of each puff is computed for a specified time-step and divided by the distance increment specified for sampling the puff. This quotient is then rounded to the next highest integer which is used as the number of times to sample the puff along the computed displacement path. During periods of high windspeeds, the puffs will be sampled several times during an advection step, but only once during sufficiently low windspeeds. When all the puffs have been displaced and sampled, the process begins again for another advection step.

To calculate the growth of each puff as it is carried by the wind, several factors are carried over from one advection step to the next. These are: the emission strength of the puffs, the σ_y- and σ_z-values for the puff, the total distance traveled by the puff, the horizontal coordinates of the puff center location, and a control parameter which indicates whether the puff has left the grid or has become so dilute that it is no longer to be considered in the calculations. The distance-dependent values of σ_y and σ_z are used to calculate the puff center concentrations. The

radius of influence of each puff is determined by the relation

$$R_p = \sigma_y \, -2 \, \ln \left[\frac{\chi_{min}}{\chi_p} \right] \qquad (8)$$

where

χ_{min} = the minimum concentration of interest

and

χ_p = the concentration at the puff center.

The concentration is computed and accumulated for each grid point which lies within the radius of influence of each puff.

It was indicated that the puffs are carried along in the computational scheme until they are totally off the grid or until their peak concentration falls below a specified level of interest. To keep the computer memory requirements to a minimum, especially for releases over an extended period of time, 400 has been set as the upper limit on the number of puffs which are carried simultaneously in the calculations. After the first 400 puffs have been released, the control parameter array is scanned; all information for the puffs, which can no longer contribute a significant concentration at any grid point, is eliminated to make room for puffs yet to be released. When the number of puffs remaining and the number subsequently released reach 400, the process is repeated. Under conditions of very low windspeed, the number of puffs simultaneously contributing to the dose may exceed 400. When more than 400 puffs exist, an attempt to eliminate noncontributing puffs occurs every hour. Under this condition, the number of puffs is allowed to grow to 500 before a message is printed and the program terminated. This termination has never occurred in several runs of 1-yr duration.

4. MODEL TESTING

A. Approximation of the Continuous Point Source

One of the concerns in the computation is whether the continuous point-source (CPS) equation is being approximated with a satisfactory degree of accuracy. If the trajectory of a plume is straight, one puff will approximate the dose pattern of a CPS to any degree of accuracy desired, provided it is sampled frequently enough as it passes each point of concern. The frequency required for the sampling will, of course, be a function of the speed of the puff and its rate of growth, which is dependent on the stability classification.

Calculations of values of total integrated concentration (TIC) were made for straight-line flow for various windspeeds and stability classes with both the puff model and the CPS equation. The most severe conditions considered for an accurate approximation were strong winds and class D stability (causes the slowest horizontal puff growth). The ratios of the TIC values for class D and a 25-m s^{-1} speed computed by the puff model and by the CPS equation for four different sampling intervals are shown in figure 1. It is apparent that to obtain reasonable accuracy to within 10 km of the source, the sampling interval should be between 1 and 2 min. In terms of puff travel distance, this is between 1.5 and 3.0 km. For this reason, the puff travel distance between samples is restricted to less than 2.4 km in the operational model. This provides a more than adequate approximation of the CPS equation for all but a few isolated cases of hourly averaged winds over 25 m s^{-1}. The operational model has been thoroughly validated against the CPS equation for straight-line flow.

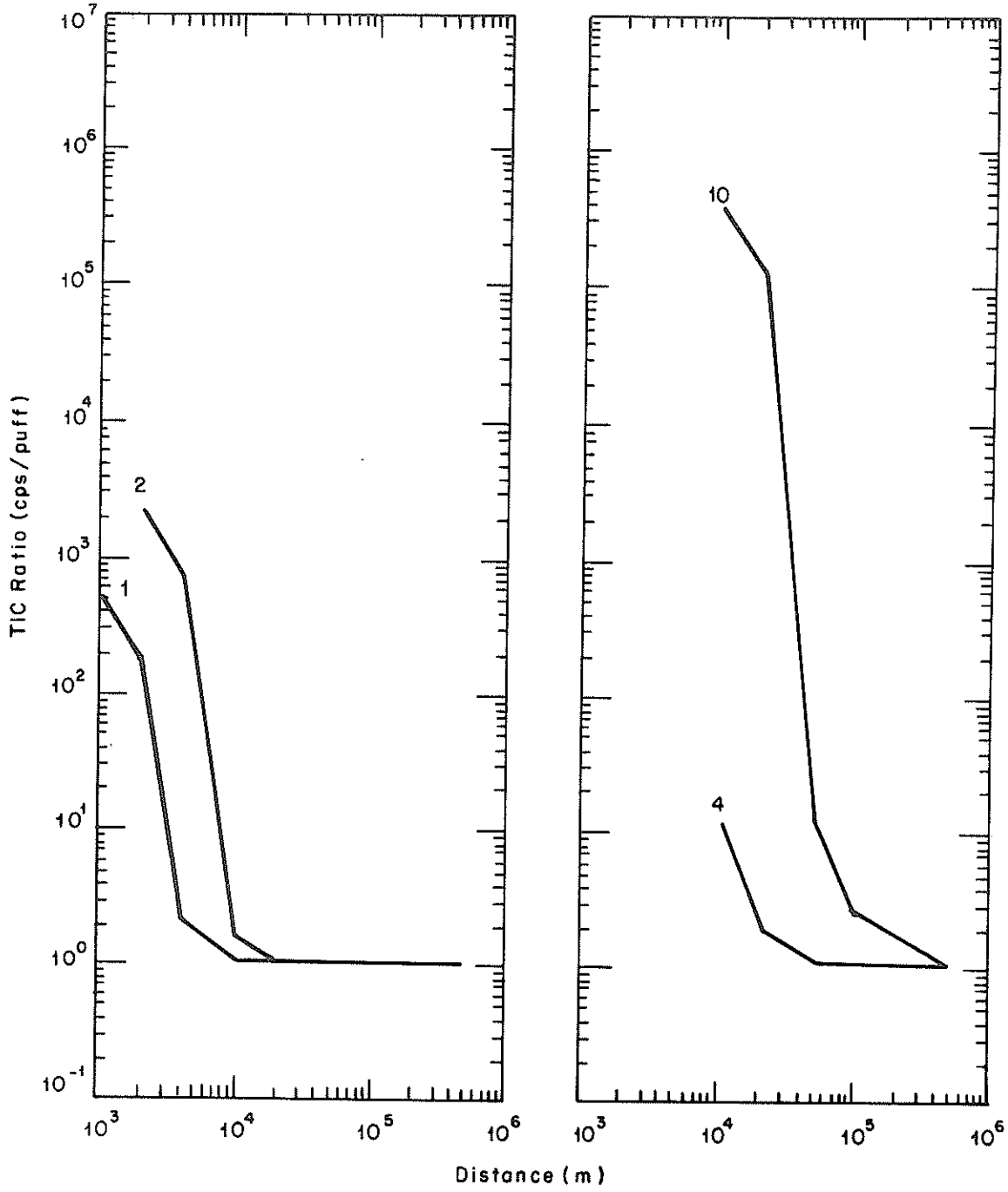

Figure 1. Ratios of total integrated concentrations (TIC) for: (a) 1- and 2-min, and (b) 4- and 10-min advection steps. All curves apply to D stability class and 25 m s^{-1} windspeed. Individual curves are labeled in minutes for different time lengths of advection steps.

B. Approximation of the Instantaneous Line Source

Because the purpose of the puff model is to handle flow with spatial variation, another major concern is that the continuous release has been divided into a sufficient number of puffs to approximate the continuous plume adequately. For example, if a series of puffs becomes oriented perpendicular to the wind and is acting as if the puffs had been released from a line source, the spacing of the puffs will strongly affect the accuracy of the approximation to a continuous plume. This is illustrated in figures 2a and 2b in which the puffs are releases at rates of three and six per hour, respectively. The dots indicate the position of the puff centers, and the circles are contours of the minimum concentration of interest. During the first 5 hr of the release shown here, the winds are steady from the southwest. This period is followed by a clockwise shifting of the wind which moves a large segment of the plume as a line perpendicular to the direction of movement. The more complete coverage of the six puffs per release (fig. 2b) is especially noticeable in the western portion of the line, beginning at 0500 Mountain Standard Time (MST).

Obviously, the greater the number of puffs per hour, the better the approximation to a continuous plume; but the computation time is almost directly proportional to the number of puffs released. To determine a compromise, the 1969 set of trajectory plots for 12-hr releases was scanned for cases in which a wind shift caused a rapid spreading of the trajectories and the phenomena of the plume moving as a line. Sets of three matrices of TICs were calculated for each case in which three, six, and 12 puffs per hour were released.

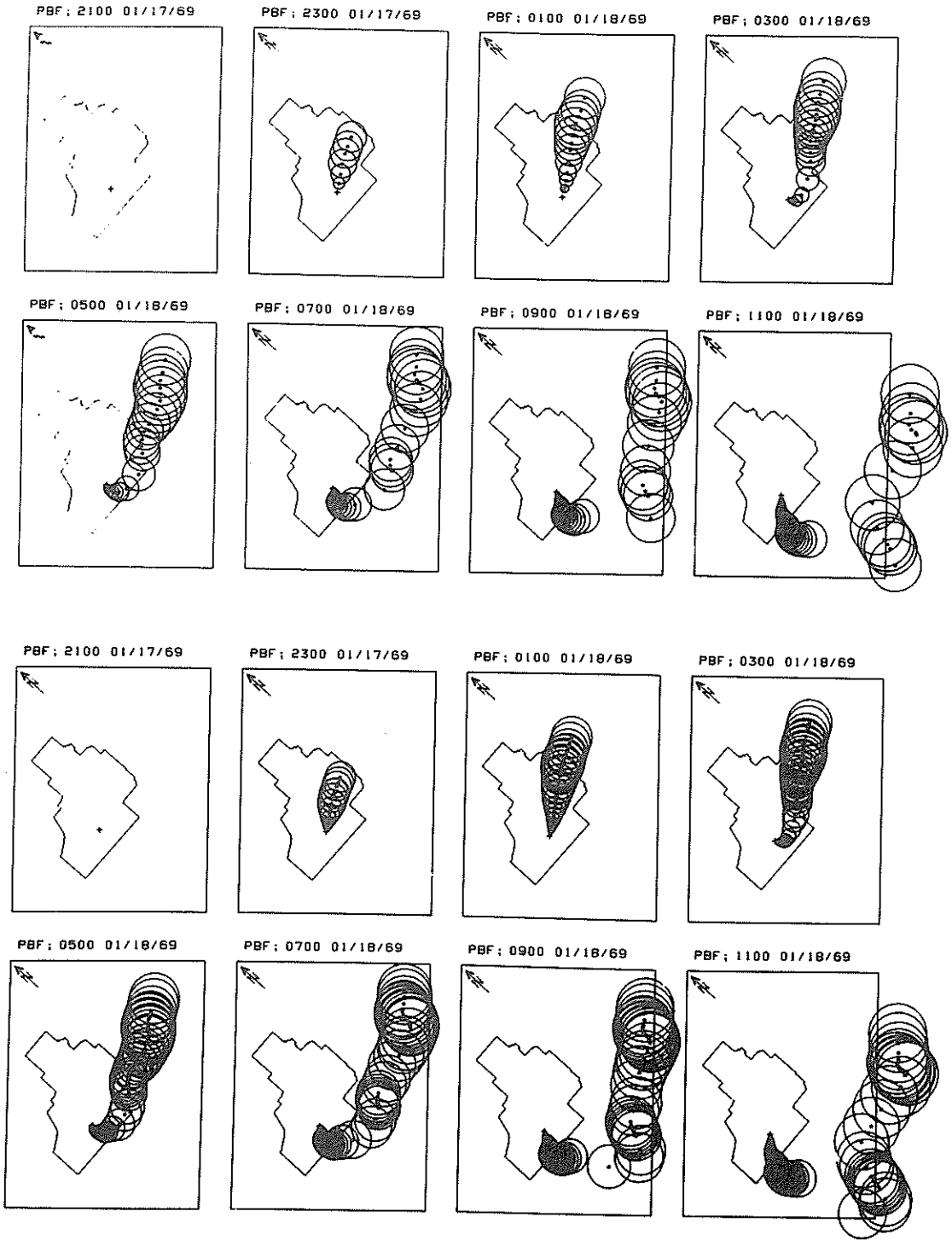

Figure 2. Plots of two hourly positions of sequentially released puffs for: (a) three puffs per hour, and (b) six puffs per hour. Each puff is depicted by a dot showing the center position and by a circle representing the contour of the lowest concentration of interest.

A comparison of the TIC matrices for each case showed that for a large percentage of the time, three puffs per hour would probably be adequate; six puffs per hour resulted in dosages which were very close to dosages resulting from 12 puffs per hour in all but the most extreme cases of wind shift. The 2100 MST release on January 17, 1969, shown in figures 2a and 2b, represents such an extreme case. As the plumes leave the southern end of the site, the puffs actually separate in both the three and six puff per hour cases. The doses in the region where the plume separates differ by a factor of two for the six- and 12-puff per hour releases. However, the actual magnitude of the doses in this region are less by two orders of magnitude than the largest doses on the grid; thus, the indication that plume segment separation is not a very serious problem. Results of these tests would indicate that a release rate of six puffs per hour should be adequate for continuous-plume approximation. For long-term releases on the order of a year, three puffs per hour would probably provide reasonable results for one-half the cost. All subsequent illustrations are based upon releases of six puffs per hour.

5. DEMONSTRATION CASES

A. Short-Term Applications

MESODIF has the potential for providing concentration or TIC values on a regional scale for an unexpected release of effluents into the atmosphere. It could be used with forecast winds for evacuation purposes or with recently recorded winds to determine the area affected since the release began. In either case, winds based on data from a network of stations would be more reliable in providing the effluent transport than data from the source wind only.

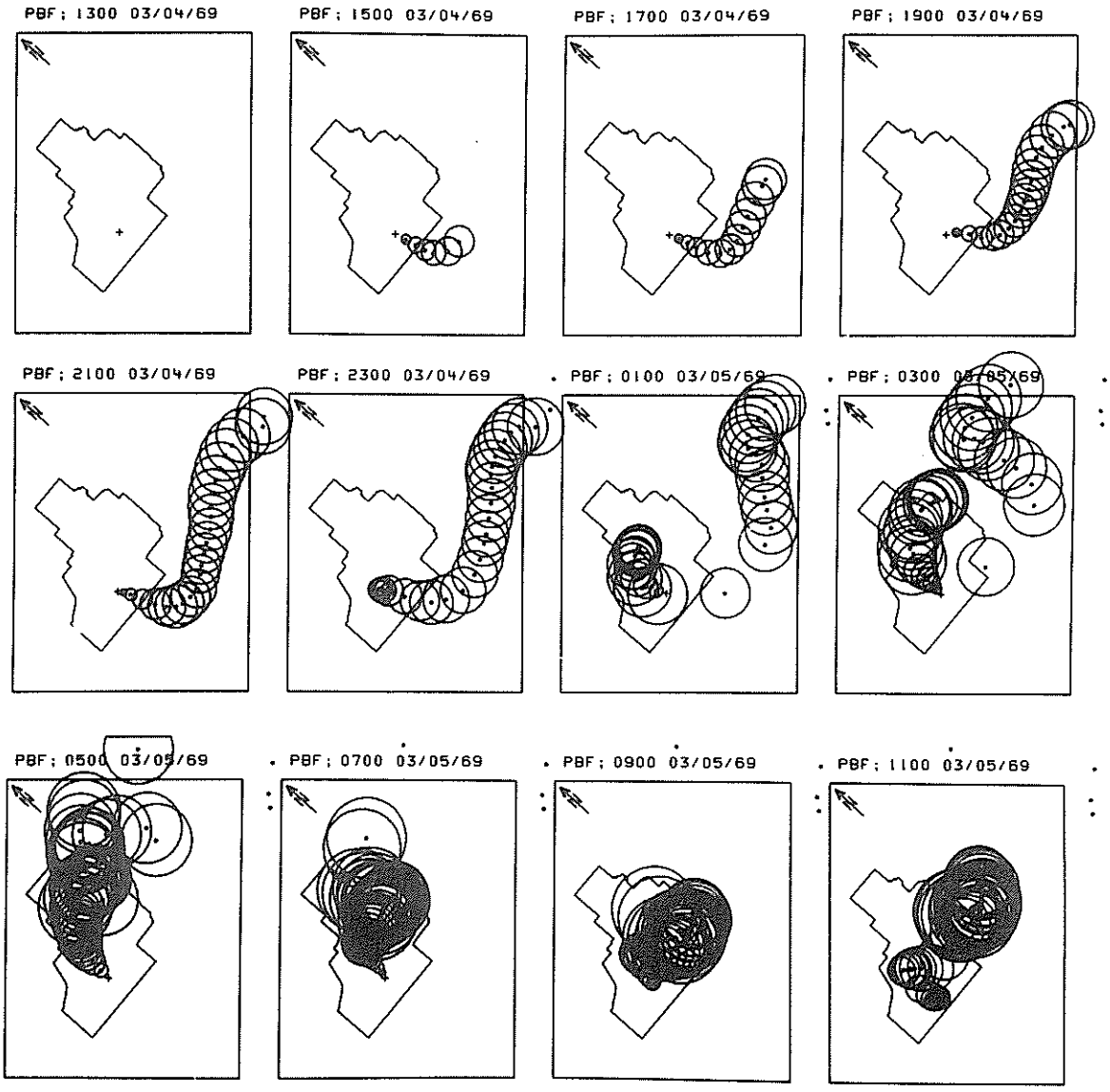

Figure 3. Plots of sequentially released puffs for a continuous release through a period in which there is much spatial and time variation in the transporting flow.

A hypothetical continuous release from a point labeled PBF was chosen as a demonstration case of the short-term application. The computer program requirements and listing are shown in appendix A and B, respectively. The release was initiated at 1300 MST on March 4, 1969, and continued for 24 hr. To put the sequence of events into perspective, two-hourly plots of the puffs (every other one) are shown in figure 3. The plus sign in the first frame indicates the location of the source. From 1300 to 2100, the puffs move away from the source in a southerly direction across the boundary of the site and then turn and move in an easterly direction for about 80 km. Between 2100 and 2300, the wind begins carrying puffs in the vicinity of the source in a northwesterly direction. By 0100, a region of strong divergence has separated the plume (approximated by the puffs) southeast of the site. The older puffs move in an arc to the east of the site and curve back around toward the northeastern site boundary; later released puffs move in a northerly direction and also turn toward the northeastern site boundary, indicating an area of convergence. By 0700, the puffs more recently emitted from the source have formed a line which sweeps from north to south across the site and is followed closely by the older puffs from the beginning of the release.

The behavior of the puffs for this release indicates a fairly complex flow pattern involving a great deal of space and time variation over the area. To show the inadequacy of the source wind in determining the transport, the six-hourly TIC contours for both wind field (WF) and single station (SS) calculations are shown in figure 4. The difference between the two calculational models is that in the SS model the hourly wind field is homogeneous over the entire grid and is based on a time series of single,

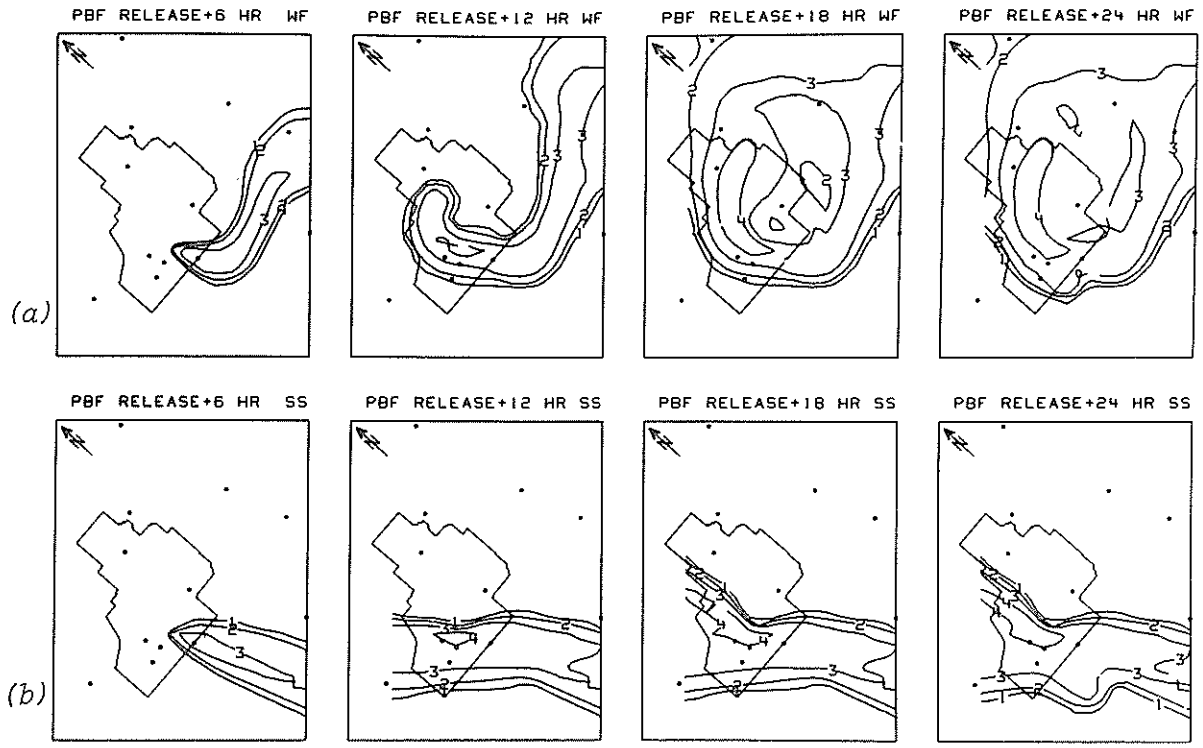

Figure 4. Contours of total integrated concentration (TIC) for the same hypothetical continuous release as is shown in figure 3, beginning at 1300 MST on March 4, 1969, from the location of the Power Burst Facility for: (a) transport based on wind field (WF) data, and (b) transport based on single station (SS) source wind data only.

hourly winds observed at the point of emission. The contrast between the TIC patterns for this case is extremely striking. The large area to the east of the site shows no effects at all for the SS transport; it is significantly affected when WF transport is considered. This difference would imply that under flow conditions of this type, an error in the diffusion calculations is far less serious than the extreme misrepresentation of the transport.

An interesting feature of this case occurred during the first 6-hr when all puffs followed essentially the same curved path, indicating that the flow over that path was not changing with time. In this instance, a forecast of no change in the WF for 1300 for the following 6 hr would have been valid; using this forecast in MESODIF would produce essentially the same dose pattern as seen in the R+6 hr (6 hr after start of release) frame of figure 4a. The same forecast of an unchanging wind at the source point would produce essentially the same pattern shown for R+6 of figure 4b. It is easily seen that longer term plans of action based on the extrapolation of the 6-hr source wind sequence could be misleading. This example is not meant to imply anything about the reliability of persistence forecasting. It demonstrates, however, that when spatial variability is present in the flow pattern, transport based on the source wind can be seriously misleading.

B. Long-Term Applications

In the case of an accidental release of an effluent into the atmosphere over a short period of time, the value of a diffusion model using a WF for the transport has been demonstrated. For continuous long-term releases, perhaps from an operating facility, a diffusion model using WF data has

has not been previously considered because of the relatively high cost of calculations and because a long record of wind data from a regional-scale network of wind stations has not been available. The most common procedure for evaluating the transport and diffusion effects from a long-term release is to use wind rose (WR) and stability data from the source location. The central assumption in this approach is that material leaving the source will travel in the direction of the source wind at the time of release until it reaches some specified boundary (the material flows radially outward within the same wind direction sector in which it began).

While this travel within sectors may not be satisfied case-by-case, the WR technique assumes that in the long-term average no systematic transverse turning of the flow occurs; losses of mass from the side of a sector are balanced by corresponding mass gains caused by an inflow from the adjoining sector. In this event, there could be a basis for use of the wind at the source to describe the distribution of effluent material at long distances for long times. In regions of topographic variations, this assumption could be invalid because of the systematic turning of the flow. This assumption will be examined in detail later.

A WR model currently being used by the AEC Directorate of Licensing (DRL) calculates χ/Q on an annual basis for various distances out to about 80 km in each wind direction sector. For a ground-level release, the rate of diffusion is a function of distance from the source, sector width, mean windspeed in the given windspeed class, σ_z with no upper bound, and the joint probability of stability, windspeed, and direction. The model is used to evaluate the dispersion potential of the atmosphere in a possible reactor site area. Initially, the model was applied to site

areas where the boundaries were only a few hundred meters from the source; for that situation, it seemed to be the most logical method. However, in areas where spatial variation in the flow patterns is frequently observed on a regional scale (Wendell, 1972), extending this method to a radius of 80 km from the source would seem to be inappropriate.

With MESODIF designed to shift noncontributing puffs out of the computer memory, it can be used to calculate a TIC pattern resulting from a continuous release of indefinite length. The postulated effluent, in the form of a string of puffs, is carried by the flow determined from the wind network until it leaves the grid or becomes too dilute to be of any more interest. The TIC information may be stored on tape in segments of any desired length; for example, week, month, or season. These segments may be examined individually or combined to produce an annual average result.

To compare the annual average TIC values for the DRL and the MESODIF models, a hypothetical ground-level continuous source was postulated at the location of the EBR II wind tower. This site was chosen because it lies nearly at the center of the mesoscale grid network. The hourly averaged winds were chosen from the 1969 data set for the network because of the extensive WF and the trajectory analysis work that has been done using this data set. The puff release rate was six puffs per hour. The same hourly stability classes were used in each model. The DRL model used a joint frequency distribution, based on the winds from the EBR II wind station and the above-mentioned hourly stability classes. The transport winds for MESODIF were calculated from the network of wind stations within the computational grid. The

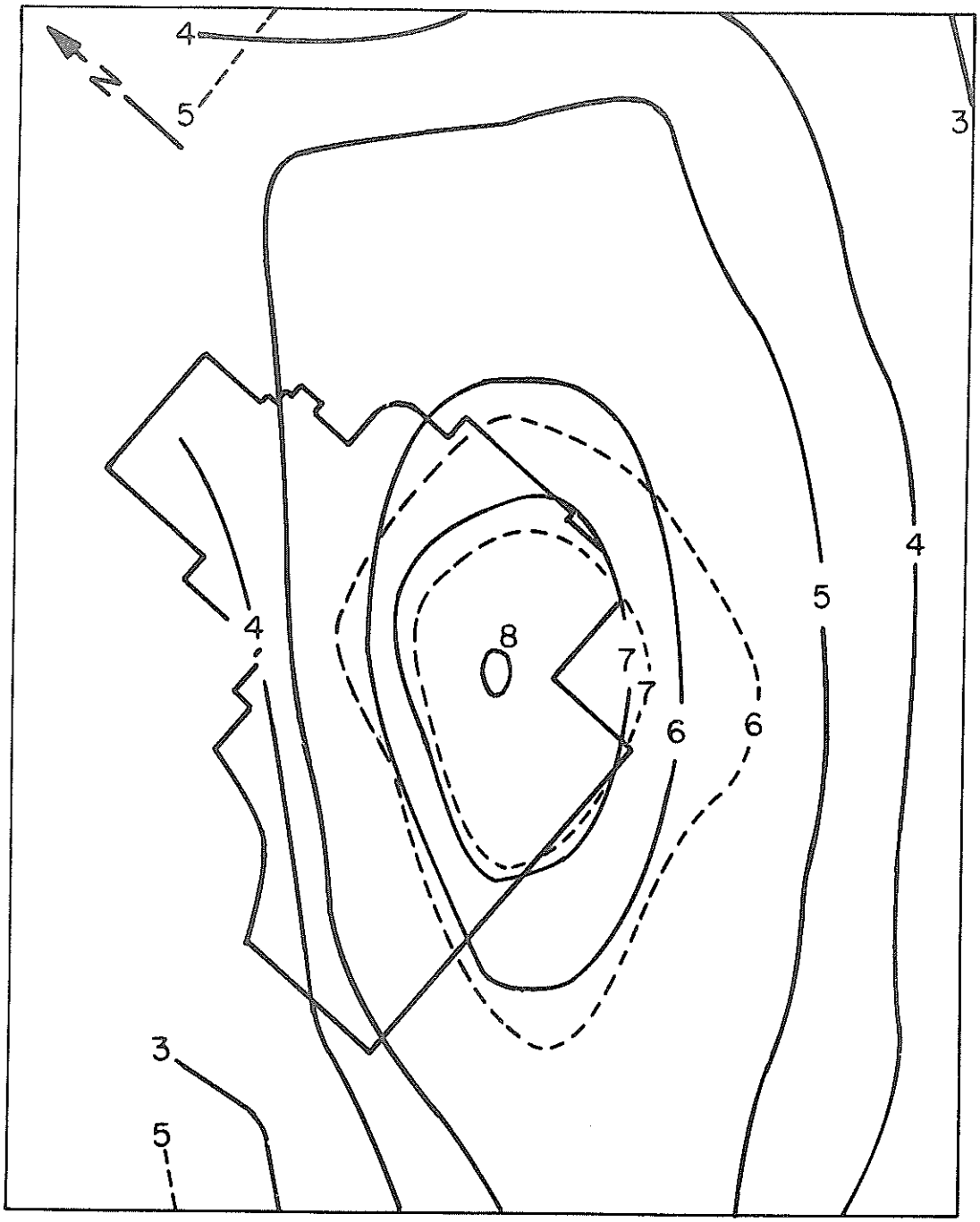

Figure 5. Contours of TIC for a continuous release from the ERB II location through the period from December 1, 1968, to November 30, 1969. The solid contours are for the MESODIF model results, and the dashed contours are for the DRL model results. Number identifiers on contour lines represent the following values. 8: $5x10^{-7}$; 7: $1x10^{-7}$; 6: $5x10^{-8}$; 5: $1x10^{-8}$; 4: $5x10^{-9}$; 3: $1x10^{-9}$; 2: $5x10^{-10}$; and 1: $1x10^{-10}$.

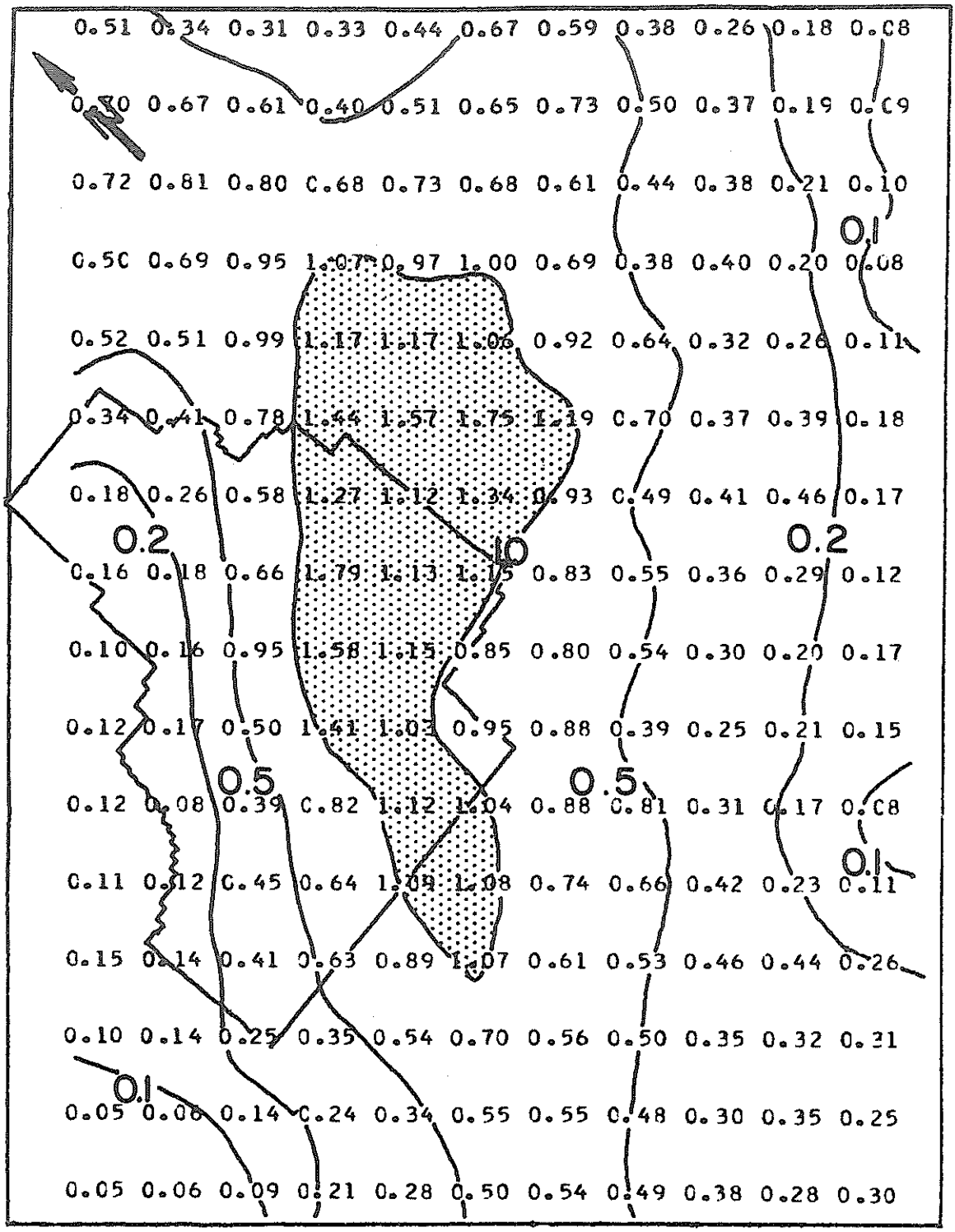

Figure 6. Ratios (MESODIF/DRL) of annual TIC values at the grid points over the computational area. Contours have been added to show the general pattern.

values of σ_z in the DRL model were calculated from equation (7) for all distances without any mixing depth restrictions. The resulting TIC values were calculated with both models for the four seasons and the entire year.

The comparison of TIC patterns for the full year is shown in figure 5. There is fairly good agreement for the first two contour levels. The shapes are basically the same with a slight southeastward shift of the DRL pattern. Within the area of these contours, the major and minor axes of diffusion appear to agree quite well. Figure 6 shows the ratios of the MESODIF/DRL TIC values at the computational grid points. The area of fair agreement is approximated by the ratios near and larger than one. Outside this 25- by 50-km area, however, the comparison is not so favorable. The TIC values from MESODIF decrease more rapidly with distance (on a logarithmic depiction) from the source, while the TIC values from the DRL model decrease at a "straight-line rate." The different rates of decrease of TIC values with distance are apparent from figure 6 which shows the MESODIF/DRL ratios decreasing to less than 0.1 at some points near the boundary. Figure 7 presents this phenomenon more quantitatively, using plots of TIC values along the major and minor axes of dispersion. The difference in the rate of decrease with distance of the TIC values from the two techniques is most apparent. Discussion of reasons for the differences will be presented in a later section .

The same type of comparisons (as shown in fig. 5 and 6) are shown for the four seasons in figures 8 and 9. The most general observations which can be made are that, on a seasonal basis, some MESODIF/DRL ratios (fig. 9) are higher than for the annual computation (up to 4.5). The

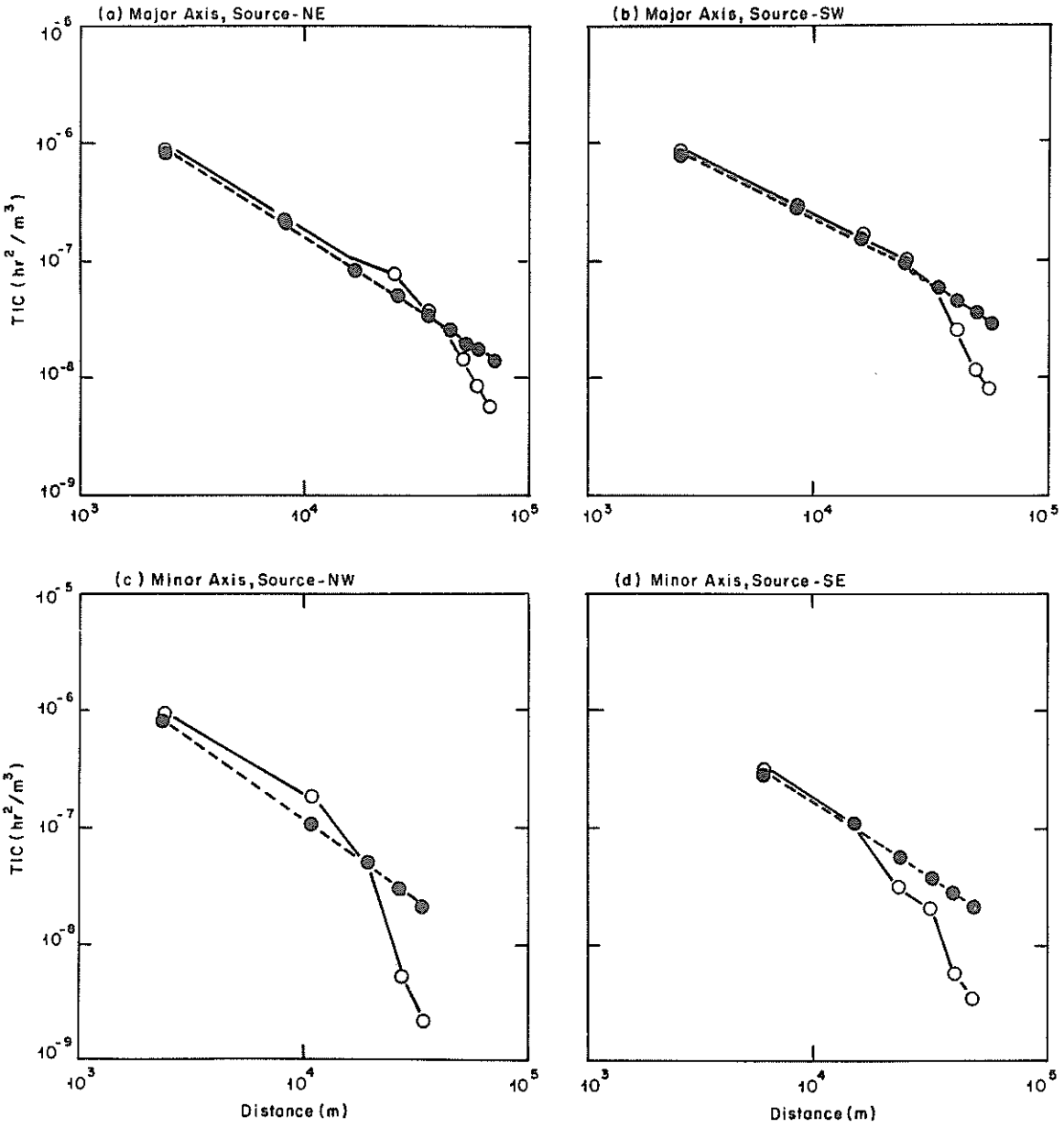

Figure 7. Plots of annual TIC against distances from the source along the major and minor axes of diffusion. The solid lines are for MESODIF results, and the dashed lines are for DRL results.

Figure 8. Seasonal contours of TIC for the same release described in figure 5. (See fig. 5 for details.) Winter is for December through February, spring is for March through May, summer is for June through August, and autumn is for September through November 1969.

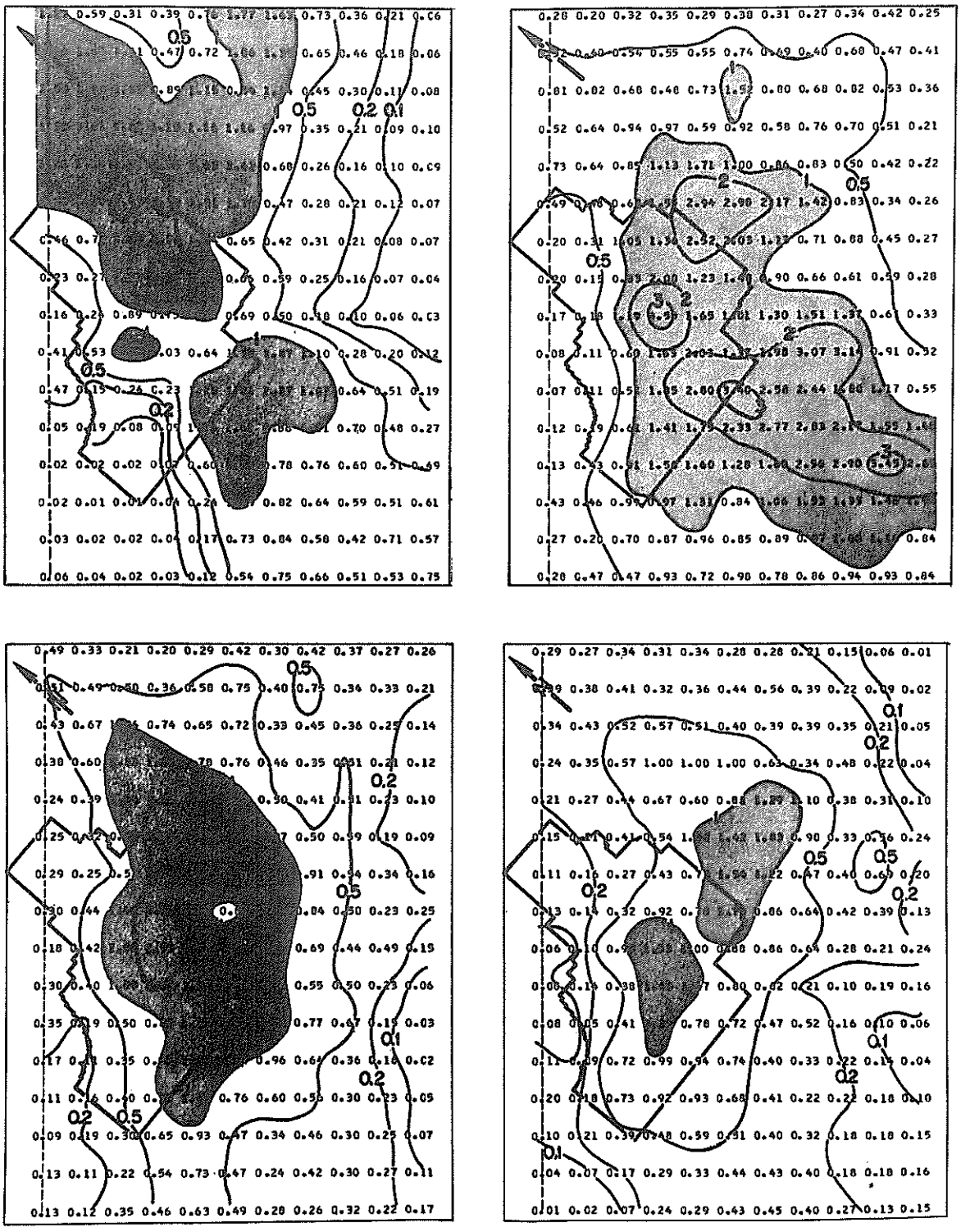

Figure 9. Seasonal ratios (MESODIF/DRL) of TIC values during the same data period are shown in figure 6. (See fig. 6 for details.)

areas of ratios greater than one show marked seasonal variability in shape and intensity. The TIC pattern comparisons in figure 9 show differences in the orientation of the major and minor axes of diffusion. Because σ-values were derived from continuous plumes with release durations of 1/2 to 1 hr, their use may have inhibited the producing of ratios greater than one within the first 2 to 10 km of the release point.

The seasonal variations in the shape of the area of the MESODIF/DRL ratios greater than one can be related to the transport as indicated by the trajectory plots. For the winter and spring seasons, these areas extend from the source to the boundaries in northeasterly and southerly directions, respectively. During the summer and autumn, these areas do not extend to any boundaries. The trajectory plots for summer and fall seasons show no particular preference for transport to any boundary; trajectory plots for winter and spring illustrate preferred zones of transport to the boundaries of the computational area.

6. DISCUSSION AND SUMMARY

Differences in areal coverages and magnitudes of total integrated concentration values have been shown in figures 4 through 9. During short release intervals (few hours) or specific case situations, the use of wind information from a single point (when spatial wind variability is present) can yield seriously misleading information if the single-point methodology were extrapolated to longer times and longer distances. Other model differences also contribute to the difference in TICs. But of all the differences, the failure to describe accurately the effluent trajectory (thereby giving a misrepresentation of the area which would be influenced) is probably the most serious error.

The extension of methodologies to regional distances and for weekly, seasonal, and yearly time intervals also retained significant residual differences in TIC estimates. However, at these extended times and distances, several factors contributed to produce the net differences illustrated in figures 5 through 9. The quantitative comparisons may be summarized as follows. The MESODIF model yielded one or more "hot spots" (regions in which TIC values were up to 4.5 times larger than the wind rose (WR) method) generally within 50 km or less of the source point. At greater distances, the WR model yielded TIC estimates about an order of magnitude greater than the MESODIF model. These differences are highly significant and should be reconciled if impact assessment calculations are to be utilized within this domain.

To understand these differences in TIC values, the models and the physical processes treated differently by each need to be reviewed. Table 1 lists six physical features treated differently in the two models. Both models treat vertical diffusion in the same manner at short distances from the source point. But when upward diffusion begins to be influenced by the presence of a capping inversion or lid, the calculated concentrations and resulting TICs begin to differ (the MESODIF values being the larger). In terms of short-distance and long-distance effects, this difference in vertical diffusion modeling should yield a region of general agreement about the source. This agreement should deteriorate with distance into a surrounding zone in which MESODIF values of TIC are progressively larger than WR values. The opposite effect is observed at the longer distances; some different process must be of greater importance.

Stagnation (or very slow speeds of transport relative to the initial source windspeed) leads to systematic increased dwell time of MESODIF

Table 1. Differences Between MESODIF and DRL/WR Models

Physical feature	Nature of influence upon long-term TICs
Vertical diffusion	Restrictive lid upon upward spreading tends to keep MESODIF TIC larger than for WR. Effect grows with distance traveled from source.
Horizontal dispersion (In the absence of terrain-related spatial variations of winds)	Two factors are considered--turbulent diffusion of effluent mass horizontally outward from the plume or puff center and dispersion of plume subelements or puffs through time changes of the horizontal wind direction. At short and intermediate times, the differences are large; at longer times, the mean directional transport differences would tend to decrease, and net results become similar at greater and greater outward distances.
Stagnation (or very low windspeeds)	MESODIF plume dwell time over receptors yields TIC values the same or greater than WR values. WR method provides a 1-hr influence at all points within the sector of the source point wind during the hour of emission. All points within a WR sector (outward to infinity) are affected by the 1-hr emission. Stagnation may be topographically influenced.
Recirculation	Not permitted by WR model. TIC values from MESODIF will be increased in regions of preferred recirculation due to repeated exposures. Terrain features could induce these effects in the wind fields.
Curved trajectories (versus straight flow outward within angular sectors)	A failure to reach distant receptors along straight-line paths outward from source point can occur. Either emission affects points outside of the sector of initial travel or fails to leave the general vicinity of source point. Failure to move far from the source is only temporary. Eventually, winds sweep the material out beyond the region of concern. In the absence of terrain influences, this effect should diminish with averaging or integrating times.
Stability changes (during times of dispersion over computational region)	By design necessity, the WR-modeled emissions reach all receptor points while having the stability category in effect during the hour of emission. MESODIF allows hour-by-hour changes of stability category as measured at source point; all emissions remaining within the computational region at the time of change then diffuse with rates specified by the new category. These influences are likely to be accumulative and most pronounced at the longer distances.

emissions over the computational region. MESODIF values of TIC will exceed WR values in these cases. In preferred zones of stagnation, TIC values would accent this difference in dwell time through successive summing of concentrations. Topography is believed to be the major source of this influence; stagnation effects may occur at any distance outward from the source point.

Recirculation, as in stagnation, would yield MESODIF values of TIC systematically larger than WR values because repeated passage of effluents over the same receptor would be analogous to longer dwell times. Again at longer distances, other factors must dominate. Terrain-related influences upon the wind flows could be expected to produce "hot spots" (MESODIF values of TIC greater than WR values) in the vicinity of those features in the topography.

Curved trajectories (rather than straight flow within a direction sector emanating outward from the source) or terrain-induced airflow channeling could produce bands or envelopes of either overestimation or underestimation of TIC values in one model versus the others. There should be compensating areas of TIC ratios so that the net difference within a source encircling-ring averages near zero. If curved trajectories exit the region from preferred areas, there must also be areas near the outer boundaries in which fewer than normal trajectories would exit. At the longer distances, the comparisons of long-term (annual) TIC values never showed MESODIF to exceed WR estimates. There may be short-distance, and certainly short-time, occurrences of this effect. However, at longer distances and times, trajectory curvature effects largely disappear and other factors still must yield those dispersion differences displayed in figure 7.

Horizontal dispersion of effluent emissions is treated differently. The WR model distributes an average concentration laterally along the arc of the sector in which the material lies. MESODIF utilizes the customary term σ_y, and concentrations decrease exponentially outward from the puff centers according to the exponential term in equation (2). When a time change of wind direction occurs, the MESODIF model includes an additional dispersion of plume effluent caused by transporting of plume segments (puffs) along different (diverging) trajectories. In the absence of terrain-induced flow variations, there should be a tendency for these diverging trajectories to average out or compensate for random divergent turning to either one side or another. At the source, this effect would be minimal for short- and long-time periods. With successively longer integrating time periods, the greater the opportunity for these random separations of trajectories to compensate and negate this effect. With longer times, the areas failing to have negated differences in diverging transport should occur only beyond progressively longer distances from the emission point. While this effect cannot be fully ruled out as a source of greater MESODIF dilutions at the longer distances, it is not believed to be a major contributor; most of the randomness should balance out.

Changes in the stability category, while MESODIF effluents released at earlier times remain within the computational area, are a major contributor to cumulative differences in longer term TIC values determined at the longer distances. By design, the WR technique prohibits the hourly effluent release from diffusing at a stability different from the hour in which it was emitted from the source; MESODIF has no such restriction. Two illustrations will help clarify the role of hour-by-hour changes in stability category in

producing systematic, additive differences. Two basic types of change in atmospheric stability category can be envisioned--change from stable to unstable and change from unstable to stable. Before proceeding, it is well to recall that atmospheric dispersion of effluents proceeds most rapidly during unstable or "daytime" conditions and least rapidly during stable or "nighttime" conditions. At distances approaching 50 km, effluent concentration estimates based upon standard empirical diffusion curves (e.g., Turner, 1970) could differ by about three orders of magnitude across the span of stability categories. A large fraction of this difference is related to the vast differences in vertical diffusion during daytime and nighttime. During daytime unstable categories, both MESODIF and WR plume effluents dilute very rapidly; their vertical dispersion would be the same until the MESODIF model experienced slower rates of dilution under the influence of a capping lid. Therefore, all other things being the same, concentrations and the resulting TIC values from MESODIF would equal or exceed values from WR during daytimes. Also, when hourly changes in stability category progress from unstable to stable, the MESODIF determined values of TIC would equal or exceed somewhat those values from the WR model. These differences are contrary to the net effect as shown in figure 7 at distances of about 50 km from the point of emission.

It is the transition from stable to unstable stability categories that yields significantly different estimates of dilution at the longer distances. The WR technique exposes all downwind receptors with concentration levels appropriate to the category of diffusion at the time of effluent emission. If the initial stability category were strongly stable, all WR model receptors downwind would be exposed to the greatest possible concentrations,

regardless of whether this atmospheric conditions would have to persist for 1/2, 10, or even 100 hr. Extremely poor dispersion conditions could conceivably persist for a sizable fraction of a day, but mean weekly, seasonal, or annual conditions certainly would not result in these extremely high TIC values at 50 to 100 km downwind from the source point. MESODIF considers hourly changes in stability category (rates of dilution). Because light windspeeds are associated with the most stable conditions, many hours of effluent transport are necessary to reach the outermost receptors. Consequently, most plume segments reaching receptors at large distances experience some periods of time in which dilution proceeds at a rapid pace. In most cases, MESODIF-modeled effluents which initially were diluting very slowly during stable conditions are rapidly diluted before reaching receptors at the longer distances. This effect is not compensated over 24 hr and longer periods of integrating time. Instead, these recurring differences in concentration estimates are systematically accumulated in the TIC values. Figures 6 and 7 clearly show these accumulated effects at the longer distances.

At distances within about 15 to 25 km, agreement of MESODIF and WR estimates was much better. In general, the two techniques either produced comparable values or MESODIF values were greater. Most of the physical processes enumerated in table 1 would tend to contribute to this type of comparison--except stability category changes.

Some insight into the development of "hot spots" at the shorter distances may be gained through examination of the local topography. Figure 10 shows this topography and has been discussed by Wendell (1972). The mountainous terrain is shown qualitatively by the shadowed relief. The gentle height variation over the relatively flat plain is depicted by height

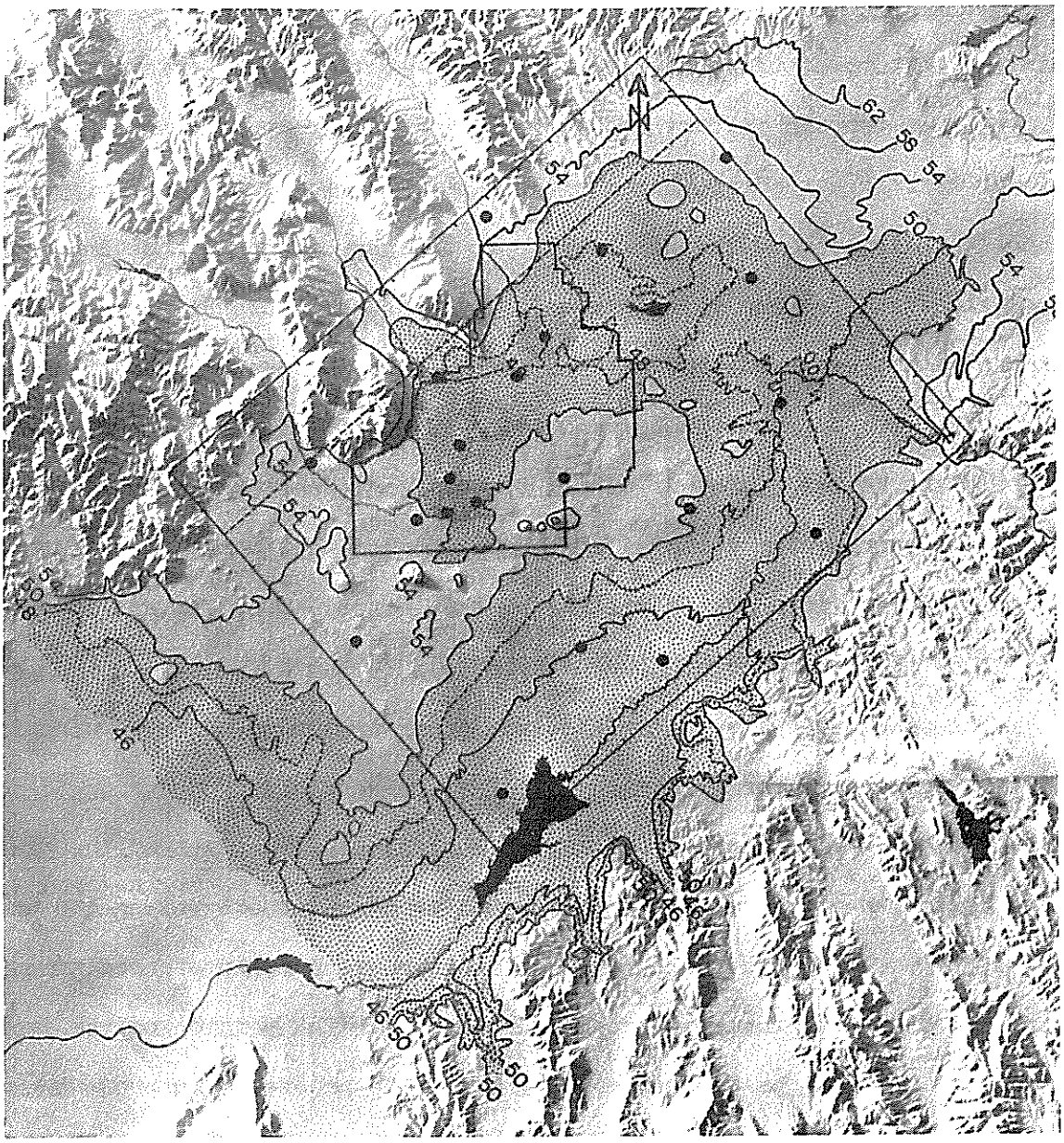

Figure 10. Relief map of the Upper Snake River Plain in southeastern Idaho. The height values of the contour lines given are in hundreds of feet above mean sea level. The stippled area indicates the area of the plain which lies below 5,000 ft. The tick marks along the grid box border indicate the computational grid mesh size, 8.6 km. The letters a, b, and c show the locations of three prominent buttes. The large dots indicate the location of tower-mounted wind sensors.

contours of feet above mean sea level (MSL). The area in which the terrain height is less than 5,000 ft MSL is stippled to emphasize an important feature of the comparatively mild terrain-height variation of the plain. The terrain feature of importance is the protruding area of slightly higher terrain extending from the west into the middle of the valley and then up-valley toward the northeast. It has the effect of creating a fish-hook-shaped depression which proceeds up along the Snake River on the right-hand side of the boxed computational area. The depression turns toward the northwest around the up-valley end of the 5,000-ft height contour and then extends toward the southwest across the National Reactor Testing Station (NRTS), the irregular bordered area. Three prominent buttes located along the protruding ridge are identified by the letters a, b, and c. The solid dots show the locations of tower-mounted wind sensors.

When the 5,000-ft contour line was superimposed on observed wind fields, varying degrees of conformity to this feature were observed during 57 percent of the days within a 1-yr sample (Wendell, 1972). Part of the time this conformance was reflected in a standing circular eddy along the up-valley edge of the protruding ridge of higher ground; a preferred area of stagnation and recirculation would be expected. The portion of the depression over the NRTS has also been observed to be an area more prone to stagnation or light and variable winds. Review of figures 6, 9, and 10 suggest a degree of conformance of the hot spots to these two areas of topographic wind influence.

In summary, the following aspects of regional effluent-dispersion calculations are points of concern and should be reconciled with whatever impact assessment schemes are to be utilized within the regional domain. For

assessments covering relatively short periods of time (such as individual cases, accidents, and intermittent operations, lasting from a few hours to a few days), the greatest single concern stems from underspecification of the detailed meteorological wind data necessary to define properly effluent trajectories and the region of potential influence. Complex, three-dimensional models may be required to describe fully impacts from accident-like emissions. A number of complex models exist, such as the particle-in-cell (PIC) types (Sklarew et al., 1971), which have been developed to describe such detailed, specific cases. However, there is one severe practical limitation common to these models; the detailed, three-dimensional meteorological data are not available on a regional scale and they are not likely to be available in the near future. From this point of view, the two-dimensional wind flow models such as MESODIF (the vertical dimension is partially treated by the limited mixing-depth concept) may be the type of practical working compromise needed for regional dispersion calculations until very detailed meteorological inputs become operationally or climatically available.

For regional assessments covering longer times, and to some extent short times, systematic terrain-related variations in the horizontal wind flows are significant. Monthly, seasonal, and annual accumulations of TIC estimates can retain residual differences compared with values determined using a single point or WR distribution of transporting winds. The WR technique is susceptible to bias toward underestimation in areas of recirculation and stagnation. At long distances, beyond about 25 to 50 km, the WR technique is likely to overpredict TICs significantly. This bias results primarily from a failure of this technique to permit modeled effluents to dilute at more rapid rates after an initially, strongly stable, stability category has modified to some category that is less stable.

The problem of a proper specification of diffusion coefficients is common to whatever method may be chosen, whether they be eddy diffusivities or Gaussian plume sigmas. Additional data are needed to extend known diffusion parameters to regional scales.

The MESODIF model and the continuous point-source equations have suitably predicted short-time (2 to 4 hr) total-integrated ground-level concentrations measured to distances near 90 km over the Upper Snake River Plain in southeastern Idaho. The meteorology of these diffusion cases was restrictively simple. Observed winds were about 15 m s^{-1} with a fairly steady wind direction. Vertical shearing of wind direction was on the order of 10° or less and the stability category was near neutral. More stringent validations of modeling techniques are needed, but to date suitable data sets for long-time periods and distances are not available.

REFERENCES

Dickson, C. R., G. E. Start, E. H. Markee, Jr., A. P. Richter, and J. Kearns (1967): Meteorology for the Loss-of-Fluid Test Reactor, 2d. Progress Report, Jan. 1966-Jan. 1967, IDO-12059, ESSA, Air Resources Field Research Office, Idaho Falls, Idaho.

Gifford, F. A. (1973): personal communication.

Sklarew, R. C., A. J. Fabrick, and J. E. Prager (1971): A particle-in-cell method for numerical solution of the atmospheric diffusion equation, and applications to air pollution problems, Final Report for the Division of Meteorology, Report No. 3SR-844-Vol. 1 APTD-0952, National Environmental Research Center, Research Triangle Park, N. C.

Slade, D. H. (ed.) (1968): Meteorology and Atomic Energy 1968, TID-24190, ESSA, Air Resources Laboratories, Silver Spring, Md., 445 pp.

Start, G. E., and E. H. Markee, Jr. (1967): Relative dose factors from long-period point source emissions of atmospheric pollutants, in Proceedings of the USAEC Meteorological Information Meeting, Chalk River Nuclear Labs., Chalk River, Ontario, Sept. 11-14, 1967, C. A. Manson (ed.), AECL-2787, pp. 59-76.

Turner, D. C. (1970): Workbook of Atmospheric Dispersion Estimates, Public Health Service Publication No. 999-AP-26, PB-191482. U. S. Dept. of Health, Education, and Welfare, Public Health Service, Div. of Air Pollution, Cincinnati, Ohio, 88 pp.

Van der Hoven, I. (ed.) (1971): Atmospheric transport and diffusion in the planetary boundary layer, June 1970-June 1971, NOAA Tech. Memo. ERL ARL-32, U. S. Dept. of Commerce, Air Resources Laboratories, Silver Spring, Md., pp. 36-46.

Wendell, L. L. (1970): A preliminary examination of mesoscale wind fields and transport determined from a network of towers, NOAA Tech. Memo. ERLTM-ARL 25, U. S. Dept. of Commerce, Air Resources Laboratories, Silver Spring, Md., 27 pp. + appendixes.

Wendell, L. L. (1972): Mesoscale wind field and transport estimates determined from a network of wind towers, Monthly Weather Rev., 100 (7): 565-578.

Yanskey, G. R., E. H. Markee, Jr., A. P. Richter (1966): Climatography of the National Reactor Testing Station, IDO-12048, U. S. Atomic Energy Commission, Idaho Falls, Idaho, 184 pp.

APPENDIX A. MESODIF COMPUTER PROGRAM REQUIREMENTS

Machine Requirements

This program and the associated subroutines are written in FORTRAN IV and use approximately 105 K bytes of memory within an IBM 360-75 computer. The running time will vary with length of release; number of puffs released per hour; and the overall dimensions, mesh size of the computational grid, and the nature of the flow pattern over the grid. The last item has to do with the number of puffs remaining on the grid to be examined at each sampling step. A 24-hr calculation, based on a continuous release rate of six puffs per hour over an 86- by 130-km grid with a mesh size of 8.6 km, takes from 10 to 18 s of computer time. Releases of this type over a 1-yr period take about 1.5 hr.

Tape or Disc Input

For the sake of efficiency, the meteorological data for this program are read in from magnetic tape or disc. The stability class and mixing depth data are read in the main program into an array called MET which contains 24 by 5 locations; each record represents 1 day's data. The format of this array is as follows:

MET(1,1) = MMDD, the first two digits denote the month and the second two the day.

MET(I,2) = Single digit from 1 to 6 denoting stability class. (I ranges from 1 to 24 indicating hour of day.)

MET(I,3) = Height of mixing depth in meters.

MET(I,4) = DDVV, DD denotes wind direction in tens of degrees and VV denotes the speed in mph. These data are not used in the version of the program presented here.

MET(I,5) = At present, this variable is a dummy but is available for use if Q is known on an hourly basis. To use it would require only a minor change in the program.

The month and day of the initiation of the release provided by the card input are used to search down the data string and bring in the proper record to begin the calculations.

The wind data used for transporting the puffs are read in by subroutine RNGRD9 into an array called IWD with a size of 24 by 31 words. Again, each record represents 1 day's data consisting of hourly averaged wind and some temperatures at the various locations in the tower network. The version of the program presented here uses only the wind data. The word IWD(1,1) contains the month and day and is used in the same fashion as MET(1,1) for obtaining the starting record. The wind data in this record are in the same format as MET(I,4). For each hour, the wind data are selected from the string by means of the variable ISKIP defined in card input section.

CARD INPUT DATA FOR MAIN PROGRAM

(All variables on cards #1-3 must be right justified)

Card	Columns	Variable	Description
1	1-5	ITIME	Time in hours for start of release
1	6-10	NRELSE	Total number of hours of effluent release
1	11-15	NSTEPS	Total number of hourly steps for current run
1	16-20	ICOLS	Number of columns in the grid
1	21-25	JROWS	Number of rows in the grid
1	26-30	NC	Dummy
1	31-35	MNST	Month in which the release is initiated
1	36-40	TDAY	Day in which release was initiated
1	41-45	TAU	Number of minutes between puff releases
1	46-50	DT	Number of minutes between each puff sampling (Used only when KVDT = 0)
1	51-55	NN1	Number of advection steps into first hour for release
1	56-60	LIMPUFF	Maximum number of puffs carried before screening out no longer contributing puffs
1	61-65	KCHIS	Store dose matrices on disc or tape at specified print intervals
1	66-70	KVDT	Allows number of minutes between puff sampling be variable as determined by speed of puff and specified minimum travel distance between sampling of puffs. KVDT = 1 variable DT, KVDT = .0 use or specified
1	71-75	KFLSH	1 - zero out dose matrix after each print and storage, 0 - allow dose matrix to accumulate
1	76-80	NTADV	Number of minutes in basic advection steps
2	16I15	PTIME(I)	I = 1,15. Hours between first 15 outputs of dose matrix. PTIME(15) will serve as time between all subsequent printouts for this run
3	All	TITLE	Title containing appropriate identification

Card	Columns	Variable	Description
			(The format for the following card is (6F10.1,4I5))
4	1-10	XSOURCE	X-coordinate of the source in Cartesian coordinates (0,0) at lower left
4	11-20	YSOURCE	Y-coordinate of the source in Cartesian coordinates (0,0) at lower left
4	21-30	DELX	Spacing in miles between grid points in the X-direction
4	31-40	DELY	Spacing in miles between grid points in the Y-direction
4	41-50	ANG	Dummy
4	51-60	CHIMIN	Minimum significant concentration value (this determines puff radius)
4	61-65	MSX	Column subscript for left boundary (for MSX = 3, X = 2)
4	66-70	MFX	Column subscript for right boundary (for MSX = 13, X = 12.0)
4	71-75	MSY	Row subscript for bottom boundary (for MSY = 1, Y = 0)
4	76-80	MFY	Row subscript for top boundary (for MSY = 16, Y = 15)

CARD INPUT DATA FOR WINDFIELD SUBROUTINE

(All numbers on the next card have to be right justified)

5	1-5	NP	Number of wind stations in the network
5	6-10	NSX	Same as MSX on card 4
5	11-15	NSY	Same as MSY on card 4
5	16-20	NFX	Same as MFX on card 4
5	21-25	NFY	Same as MFY on card 4
5	26-30	NSTL	Limit on number of stations to be used in interpolation if limiting radius has been reached
5	31-35	INPT	Source of wind data, 1 - tape, 0 - disc
5	36-40	NSKIP	Number of records to skip before beginning input of wind data

Card	Cols. or Format	Variable	Description
6	1-10	RTE	Angle, in degrees, of grid rotation from north
6	11-20	RCH	Radius, in grid units, within which all stations are to be used in interpolation
7	16F5.0	X(I)	X-coordinate of each station (I = 1,NPA)
8	16F5.0	Y(I)	Y-coordinate of each station (I = 1,NP)
9	16F5.0	COR(I)	Corrections, if any, in degrees to wind direction (I = 1,NP)
10	16F5.0	CONFAC(I)	Multiplier of windspeed to adjust for height of sensor. Log profile may be used to adjust data to same height. If no adjustment desired, use one
11	16(1XA4)	NAMST(I)	One- to four-character identification of each station (I = 1,NP)
12	31I2	ISKIP(I)	Control parameter to extract selected information from data record (I = 1,31). 1 - use data, 0 - bypass
13	16A4	KMON(I)	Three-character month identifiers
14	1-2	YEAR	Two-digit year identification
15	1-5	MS	Month in which release begins
15	6-10	IDS	Day in which release begins
15	11-15	IHS	Hour in which release begins

APPENDIX B. MESODIF COMPUTER PROGRAM LISTING

```
C    MESCDIFF
C
C    PROGRAM TO COMPUTE RELATIVE CONCENTRATION FOR RECIRCULATION OF
C    EFFLUENT--MULTIPLE PUFFS SIMULATE A CONTINUOUS RELEASE OF EFFLUENT--
C
      DIMENSION XS(40),YS(40),CHI(26,32),SGY(500),Q(500),
     1DXS(500),DYS(500),XP(500),YP(500),STOTAL(500),
     2MF(500),SIGZ(500),TITLE(20),PTIME(15)
      DIMENSION UU(13,16),VV(13,16),U(13,16),V(13,16),US(2),VS(2)
      DIMENSION XG(2),YG(2),DX(2),DY(2)
      INTEGER*2 MET(24,5)
            INTEGER TPUFFS,TTIME,THOUR,TDAY,STAB,TAU,DT,QC,TITLE,PTIME
      NRD=1
    2 FORMAT (5F10.0,E10.0,4I5)
    3  FORMAT(3I10)
    5  FORMAT(6H1A(N)=E10.3,5X,5H DXN=E10.3,5X,5H DYN=E10.3,5X,6H U(N)=E
     110.3,5X,5H PHI=E10.3,8H LDEPTH=E10.3)
    7  FORMAT(34X,7H ITIME=I3,08X,7H NSTOP=I4,08X,8H NSTEPS=I4,08X,7H IC
     1OLS=I3/34X 7H JROWS=I3,10X,4H NC=I4,06X,16H PRINT INTERVAL=I3,05X,
     26H TDAY=I3/34X 6H TAU =,I3,5H DT =,I3,'   NTADV=',I3)
    8  FORMAT(34X,8H XSOURC=  E10.3,7X,8H YSOURC=  E10.3,8X,6H DELX=  E1
     10.3/34X,6H DELY=  E10.3,9X,5H ANG=  E10.3,9X,8H CHIMIN=  E10.3,/
     24I5)
    9  FORMAT(/39X,16H OUTPUT OF TABLE/34X,7H  HOUR ,01X,10H STABILITY
     1                              ,7H LDEPTH/(30X,2I9,3X,I9))
   10  FORMAT(I5,8E14.5)
   11  FORMAT(/61X,9H Q VALUES/(10X,8E14.5))
   13  FORMAT(2H0 ,16H Y COORDINATE OF,25X,32H X COORDINATE OF THE GRID
     1POINTS/2X,16H THE GRID POINTS,I8,9I10/)
   14  FORMAT(I11,8X,10E10.2)
   15  FORMAT(2H 2,9H PAGE NO.I3,24X,56H DOSE FACTOR ACCUMULATED FROM AL
     1L HOURLY PACKETS FOR THE/39X,I2,15H TH DAY AND THEI5,10H TH HOUR (
     2I5,' HOURS AFTER RELEASE)'/39X,I5,' HOURS AFTER LAST FLUSH')
   20 FORMAT (20A4)
   21  FORMAT(1H0,28X,20A4)
   23  FORMAT(8E10.1)
   24  FORMAT(51H ANGLE OF ROTATION GREATER THAN 90 OR LESS THAN -90)
   28  FORMAT(46H X AND-OR Y COORDINATES OF SOURCE ARE OFF GRID)
       NS = 0
   50  READ 702, ITIME,NRELSE,NSTEPS,ICOLS,JROWS,NC,MNST,TDAY,TAU
     1,  DT,NN1,LIMPUF,KCHIS,KVDT,KFLSH,NTADV
  702  FORMAT(16I5)
       READ 703,FMSH
  703 FORMAT (F5.0)
       KFMSH=FMSH+.2
       KK=NRELSE
       IHR=ITIME
       IDAY=TDAY
       IMON=MNST
       NU=450
       READ 702,(PTIME(I),I=1,15)
```

```
      KN=0
      KJ=0
      NPD=0
      CDIST=1.5/5.3333
      FTAU=TAU
      KLGK=0
   45  READ(5,20)  TITLE
       READ(5,2) XSOURC,YSOURC,DELX,DELY,ANG,CHIMIN,MSX,MFX,MSY,MFY
      IF(KFMSH.EQ.1) GO TO 704
      ICOLS=ICOLS*2-1
      JROWS=JROWS*2-1
      NSX=MSX*2-1
      NSY=MSY*2-1
      NFX=MFX*2-1
      NFY=MFY*2-1
      GO TO 705
  704 NSX=MSX
      NSY=MSY
      NFX=MFX
      NFY=MFY
  705  XSB=MSX-1
       XLB=MFX-1
       YSB=MSY-1
       YLB=MFY-1
       KTM=0
C**** EVALUATION OF CONSTANTS FOR COMPUTATIONS IN GRID UNITS
      CGXM=1609.35*DELX
      CGX=CGXM/FMSH
      CGXI=1./CGXM
      CGX2=-0.5*CGX**2
       NSTOP=ITIME+NRELSE
C   MAXIMUM HOURS OF RELEASE IS NRELSE
  552  WRITE(6,21)  TITLE
       WRITE(6,7) ITIME,NSTOP,NSTEPS,ICOLS,JROWS,NC,IPRINT,TDAY,TAU,DT,
     1INTADV
       WRITE(6,8)XSOURC,YSOURC,DELX,DELY,ANG,CHIMIN,MSX,MFX,MSY,MFY
      TESTDT=MOD(60,DT)
      IF(TESTDT) 910,9738,910
  910 PRINT 911
  911 FORMAT (1HO,20X,'DT IS NOT A FACTOR OF 60')
      GO TO 40
 9738 TAUCHK=MOD(60,TAU)
      IF(TAUCHK) 912,9739,912
  912 PRINT 913
  913 FORMAT (1HC,20X,'TAU IS NOT A FACTOR OF 60')
      GO TO 40
 9739 NCNTRL=TAU/DT
      IF(NCNTRL.GE.1) GO TO 58
      PRINT 9071
 9071 FORMAT (20X,'DT IS LARGER THAN TAU')
      GO TO 40
```

```
   58  IF(ANG.GT.90.0.OR.ANG.LT.(-90.0)) GO TO 908
   59  NS = NS + 1
       TPUFFS = 0
       MSUM = 0
       TTIME = ITIME
       COLS = ICOLS - 1
       ROWS = JROWS -1
       IF(XSOURC.GT.XLB.OR.XSOURC.LT.0.0.OR.YSOURC.GT.YLB.OR.YSOURC.LT.0
     1.0) GO TO 904
C      CODEING TO SET UP MATRIX PRINTOUT FORMATS
   65  NP = (ICOLS - 1) / 10 + 1
       LL = (ICOLS + NP - 1) / NP
C      CODEING TO CALCULATE DISTANCES OF GRID POINTS
       DO 76 J=1,JROWS
      YS(J)=J-1
       DO 76 I=1,ICOLS
       CHI(I,J) = 0.0
   76  CONTINUE
       DO 78 I=1,ICOLS
   78 XS(I)=I-1
       II = 1
       PRSTAB = 0
      NEL=1
      IDIOT = PTIME(NEL)
       SZMAX = 0.1
       NPH=60/TAU
      NADV=60/NTADV
      KPFCHK=MOD(NADV,NPH)
      IF(KPFCHK.EQ.0) GO TO 85
      PRINT 80,NADV,NPH
   80 FORMAT ('0 BAD SPECIFICATION OF ADVECTION AND RELEASE STEPS,NADV='
     1,I5,'   NPH=',I5)
      STOP
   85 KPFS=NADV/NPH
      FADV=NTADV
      DTT=1./FLOAT(NPH)
      NPH1=NPH+1
      DTH=FLOAT(DT)/60.
      NDT=NTADV/DT
      FNDT=NDT
      ADT=1./FLOAT (NADV)
      FAC=ADT/DELX
      ACNST=2.*DTH/(6.283185**1.5)
      BCNST=2./(60.*6.283185**1.5)
      SYX=20000.
      CHMN=(CHIMIN/60.)*FLOAT(KPFS)
      CHIMIN=CHIMIN*DTH*FLOAT(KPFS)
      DTS=60.*FLOAT(DT)
      KS=0
      QNPH=1./FLOAT(NPH)
      TPUFFS=0
```

```
      MOFG=C
      PRINT 9085,NADV,KPFS
 9085 FORMAT (' NADV=',I3,'    KPFS=',I3)

C**** LOCATION OF STARTING RECORD OF MIXING DEPTH AND STABILITY DATA
   98 READ (9) MET
      MTII=MET(1,1)
      MMON=MTII/100
      IF(MMON.NE.MNST) GO TO 98
      MDAY=MTII-MMON*100
      IF(MDAY.NE.IDAY) GO TO 98
 9999 PRINT 99,MET(1,1),(MET(I,2),I=1,24)
   99 FORMAT (1X25I5)
      ITS=ITIME-1
      IHTT=C
C
C    LOOP THRU TIME STEPS
  100  DO 600 N=1,NSTEPS
      IHTT=IHTT+1
      ITS=ITS+1
      IF(ITS.LE.24) GO TO 115
      READ (9) MET
      PRINT 99,MET(1,1),(MET(I,2),I=1,24)
      ITS=1
  115 STAB=MET(ITS,2)
      LDEPTH=MET(ITS,3)
      CGLDP=FLOAT(LDEPTH)
       GO TO (131,132,133,134,135,136), STAB
C      EMPIRICAL NRTS COEFFICIENTS FOR SIGY AND SIGZ CALCULATIONS
  131  A = 0.718
       B = 0.100
       QG = 1.033
      QGI=0.968
       GO TO 137
  132  A = C.425
       B = 0.105
       QG = 0.975
      QGI=1.026
       GO TO 137
  133  A = 0.349
       B = 0.128
       QG = 0.891
      QGI=1.122
       GO TO 137
  134  A = 0.267
       B = 0.146
       QG = 0.824
      QGI=1.214
       GO TO 137
  135  A = 0.299
       B = 0.331
```

```
       QG = 0.567
      QGI=1.764
       GO TO 137
  136  A = 0.401
       B = 0.812
       QG = 0.307
      QGI=3.257
  137  CCHGPT = 0.335 * CGLDP
       SZSMAX = 0.465 * CGLDP
       SMAX = (SZSMAX / B) ** QGI
       SZMAX  = 0.8   * CGLDP
      A85=0.85*A
      A16=16.0769*A
      NPCH=NN1
      IF(TPUFFS.LT.LIMPUF) GO TO 139
C**** SECTION TC REMOVE PUFFS WHICH HAVE LEFT THE GRID
      I=1
      J=1
  340 IF(MF(I).EQ.0) GO TO 350
      MF(J)=MF(I)
      SGY(J)=SGY(I)
      Q(J)=Q(I)
      STOTAL(J)=STOTAL(I)
      SIGZ(J)=SIGZ(I)
      XP(J)=XP(I)
      YP(J)=YP(I)
      DXS(J)=DXS(I)
      DYS(J)=DYS(I)
      J=J+1
  350 I=I+1
      IF(I.LE.TPUFFS) GO TO 340
      JS=J-1
      JPOF=TPUFFS-JS
      PRINT 360,JPOF,JS
  360 FORMAT (1HO,I5,' PUFFS DROPPED   ',I5,' PUFFS LEFT')
      TPUFFS=JS

C**** LOOP THRU ADVECTION STEPS FOR THE HOUR
  139  DO 500 NN=NN1,NADV
      TINCS=FLOAT(NN-1)*ADT
      IF(N.GT.NRELSE) GO TO 150
      IF(NN.NE.NPCH) GO TO 150
      NPCH=NPCH+KPFS
  141 TPUFFS=TPUFFS+1
      IF (TPUFFS.LT.500) GO TO 142
      PRINT 9142, TPUFFS
 9142 FORMAT('1 TPUFFS ',I5  ,' EXCEEDS DIMENSION')
      STOP
  142 CONTINUE
      MF(TPUFFS)=1
      SGY(TPUFFS)=1.
```

```
      XP(TPUFFS)=XSOURC
      YP(TPUFFS)=YSOURC
      Q(TPUFFS)=QNPH
      STOTAL(TPUFFS)=0.000156
      SIGZ(TPUFFS)=.000012

C**** LOOP THRU ALL PUFFS
  150  DO 500 M=1,TPUFFS
      IF(MF(M).EQ.0) GO TO 500
      TINC=TINCS
      QM=Q(M)
      STOTLM=STOTAL(M)
      SIGZM=SIGZ(M)
      XPM=XP(M)
      YPM=YP(M)
      SIGY=SGY(M)
      IF(XPM -XSB) 155,155,143
  143 IF(XPM -XLB) 144,144,155
  144 IF(YPM -YSB) 155,155,145
  145 IF(YPM -YLB) 146,155,155
  146 MOFG=0
      IF(KTM) 205,205,210
  205 KTM=KTM+1
      NNS=1
C**** DTIME= TIME IN HOURS BETWEEN MAPS
      DTIME=1.
      CALL RNGRD9(KN,KJ,IHR,IDAY,IMON,U,V)
  515  CONTINUE
       GO TO 211
  210 IF(NN-NNS) 206,201,201
  206 DO 411 I=MSX,MFX
      DO 411 J=MSY,MFY
      U(I,J)=UU(I,J)
  411 V(I,J)=VV(I,J)
  211 CALL RNGRD9(KN,KJ,IHR,IDAY,IMON,UU,VV)
  201 XG(1)=XPM
      YG(1)=YPM
      DO 43 K=1,2
      FM=K
      C2= (TINC + (FM-1.) *ADT)
      C1=1.0-C2
      I=XG(K)+1.
      IF (I.LT.MSX) GO TO 29
      IF (I.GE.MFX) GO TO 29
      J=YG(K)+1.
      IF (J.LT.MSY) GO TO 29
      IF (J.GE.MFY) GO TO 29
      FI=I-1
      FJ=J-1
      RX=XG(K)-FI
      RY=YG(K)-FJ
```

```
      I1=I+1
      J1=J+1
      RX1=1.-RX
      RY1=1.-RY
      AA=RX1*RY1
      BB=RY*RX1
      C=RX*RY
      D=RX*RY1
      CST=AA*(C1*U(I,J)+C2*UU(I,J))
      CST=CST+BB*(C1*U(I,J1)+C2*UU(I,J1))
      CST=CST+C*(C1*U(I1,J1)+C2*UU(I1,J1))
      CST=CST+D*(C1*U(I1,J)+C2*UU(I1,J))
      US(K)=CST
      CST=AA*(C1*V(I,J)+C2*VV(I,J))
      CST=CST+BB*(C1*V(I,J1)+C2*VV(I,J1))
      CST=CST+C*(C1*V(I1,J1)+C2*VV(I1,J1))
      CST=CST+D*(C1*V(I1,J)+C2*VV(I1,J))
      VS(K)=CST
      DX(K)=US(K)*FAC
      DY(K)=VS(K)*FAC
      IF (K-2) 34,43,34
   34 MM=K+1
      XG(MM)=XG(K)+DX(K)
      YG(MM)=YG(K)+DY(K)
   43 CONTINUE
      DXM=0.5*(DX(1)+DX(2))
      DYM=0.5*(DY(1)+DY(2))
      GO TO 230
   29 MOFG=1
  230 NNS=NN
  280 CONTINUE
      IF(MOFG) 153,153,155
  153 DXS(M)=DXM
      DYS(M)=DYM
      GO TO 157
  155 DXM=DXS(M)
      DYM=DYS(M)
  157 DS=SQRT (DXM**2+DYM**2)
      IF(KVDT.EQ.0) GO TO 158
      NDT=DS/CDIST+0.5
      IF(NDT.LT.1) NDT=1
      IF(NDT.GT.5) NDT=5
      FNDT=NDT
      TNDT=FADV/FNDT
      ACNST=BCNST*TNDT
      CHIMIN=CHMN*TNDT
  158 DS=DS/FNDT
      DXM=DXM/FNDT
      DYM=DYM/FNDT
      K20=1
      IF(STOTLN.LT.SYX) K20=0
```

```
      DSMTR=DS*CGXM
      DSMHF=DSMTR*0.5

C**** LOOP THRU THE NUMBER OF SAMPLING STEPS DURING THE ADVECTION STEP
      DO 494 JN=1,NDT
       STOTLM = STOTLM + DSMTR
      SMDL=STOTLM-DSMHF
C   CALCULATE SIGZ AND SIGY
       IF(SIGZM.GE.SZMAX) GO TO 168
  161  IF(SIGZM.GE.SZSMAX) GO TO 165
C   IF SIGZ(M) GE SZSMAX USE LINEAR FORMULA
C   IF SIGZ(M) LT SZSMAX USE POWER FORMULA
  162  TERM96 = SIGZM / B
       TERM98 = TERM96 ** QQI *DSMTR
       TERM99 =(TERM98 - SMAX)/ SMAX
       IF(TERM99)  163,164,164
  163  DELTA= B * (TERM98 ** QQ - TERM96)
C   POWER FORMULA
       GO TO 166
  164  SIGZM = SZSMAX
C   POWER TO LINEAR FORMULA CHANGE DURING THIS TIME INTERVAL
       DELTA = CCHGPT * TERM99
       GO TO 166
  165  DELTA=(DSMTR/SMAX)*CCHGPT
C   LINEAR FORMULA FOR COMPUTING DELTA FOR SIGZ
  166  SIGZM = SIGZM + DELTA
       IF(SIGZM.LE.SZMAX) GO TO 168
  167  SIGZM = SZMAX
  168 IF(M.LT.IPUFFS) GO TO 1681
      SIGY=A*STOTLM**0.85
      GO TO 175
 1681 IF(STOTLM.GT.SYX) GO TO 1682
      SIGY=SIGY+A85*DSMTR/SMDL**0.15
      GO TO 175
 1682 IF(K20.EQ.1) GO TO 1683
      K20=1
      ST1=STOTLM-DSMTR
      DS1=SYX-ST1
      DS2=STOTLM-SYX
      SMDL=ST1+DS1*0.5
      SIGY=SIGY+A85*DS1/SMDL**0.15
      SMDL=STOTLM-DS2*0.5
      SIGY=SIGY+A16*DS2/SQRT(SMDL)
      GO TO 175
 1683 SIGY=SIGY+A16*DSMTR/SQRT(SMDL)
C   CALCULATE RADIUS OF PUFF(RP) AND COORDINATES OF PUFF
  175  SIGYSQ = SIGY * SIGY
      HSGSQ=CGX2/SIGYSQ
  178 PUFCHI=QM*ACNST/(SIGYSQ*SIGZM)
  179  IF (PUFCHI.LE.CHIMIN) GO TO 194
  180  PCDT = PUFCHI
```

```
      RP=SIGY*SQRT(-2.*ALOG(CHIMIN/PCCT))*CGXI
      XPM=XPM+DXM
      YPM=YPM+DYM
C   CHECK IF PUFF HAS MOVED OFF GRID
      IF(XPM+RP.LT.XSB) GO TO 194
  191 IF(XPM-RP.GT.XLB) GO TO 194
  192 IF(YPM+RP.LT.YSB) GO TO 194
  193 IF(YPM-RP.LE.YLB) GO TO 200
  194  MF(M) = 0
      GO TO 500
C
C**** DETERMINATION OF CONTRIBUTIONS TO SURROUNDING GRID POINTS
  200 RP=RP*FMSH
      XPN=XPM*FMSH
      YPN=YPM*FMSH
      RPSQ=RP**2
      ISTRT=XPN-RP+2
      ISTP=XPN+RP+1
      JSTRT=YPN-RP+2
      JSTP=YPN+RP+1
      IF(ISTRT.LT.NSX) ISTRT=NSX
      IF(ISTP.GT.NFX) ISTP=NFX
      IF(JSTRT.LT.NSY) JSTRT=NSY
      IF(JSTP.GT.NFY) JSTP=NFY
 9991 DO 320 I=ISTRT,ISTP
      XD2=(XPN-XS(I))**2
      DO 310 J=JSTRT,JSTP
      YD2=(YPN-YS(J))**2
      RSQ=XD2+YD2
      IF(RSQ.GT.RPSQ) GO TO 310
      PCHI=PCCT*EXP(HSGSQ*RSQ)
 9995 FORMAT ('      I=',I3,'    J=',I3,'    PCHI=',E13.6,9F9.4)
  309 CHI(I,J)=CHI(I,J)+PCHI
  310 CONTINUE
  320 CONTINUE
  494 CONTINUE
  499 SIGZ(M)=SIGZM
      SGY(M)=SIGY
      STOTAL(M)=STOTLM
      XP(M)=XPM
      YP(M)=YPM
  500  CONTINUE
      NN1=1
      IF(N.GT.KK.AND.MSUM.LE.0) GO TO 525
  524 IF (N.NE.NSTEPS.AND.N.NE.IDIOT) GO TO 560
  525 MSUM=0
      DO 505 MM=1,TPUFFS
  505 MSUM=MSUM+MF(MM)
      PRINT 9996
 9996 FORMAT (1H1)
      PRINT 510,MSUM
```

```
  510 FORMAT (1HO,I6,'  PUFF(S) REMAINING')
      CHI(1,1)=IHR
      CHI(1,2)=IDAY
      CHI(1,3)=IMON
      CHI(1,4)=IHTT
       DO 540 L=1,NP
      IL=L
       L2 = L * LL
       L3 = L2 - LL
       IF(L2.LE.ICOLS) GO TO 531
  530  L2 = ICOLS
  531  L3 = IABS(L3)
       L1 = L3 + 1
       L4 = L2 - 1
      IF(L.GT.1) GO TO 545
       WRITE (6,21)(TITLE(I),I=1,14)
       WRITE(6,15)IL,TDAY,ITS,N,IHTT
  545  WRITE(6,13) (I,I=L3,L4)
       DO 541 J=1,JROWS
       JJ=JROWS-J
      J1=JJ+1
       WRITE(6,14) JJ,(CHI(I,J1),I=L1,L2)
  541  CONTINUE
  540  CONTINUE
C**** SECTION TO SAVE CHI MATRIX ON DISK, THEN CLEAR IT OUT
      IF(KCHIS.EQ.0) GO TO 449
      WRITE (10) CHI
  449 IF(KFLSH.EQ.0) GO TO 452
      DO 450 I=1,ICOLS
      DO 450 J=1,JROWS
  450 CHI(I,J)=0.
      IHTT=0
  452 TMIN=C.0
 5449 NEL = NEL+1
      IF (NEL.GE.15) GO TO 5453
 5451 IF (PTIME(NEL).EQ.0.) GO TO 5453
 5452 NUT=PTIME(NEL)
 5453 IDICT = IDIOT+NUT
  560  TTIME =ITIME + N
      IF(N.GT.KK.AND.MSUM.LE.0) GO TO 40
  600  CONTINUE
      GO TO 40
  904 PRINT 28
      GO TO 40
  908 PRINT 24
   40 STOP
      END
```

```
      SUBROUTINE RNGRD9 (KN,KJ,III,IDAY,MCN,UG,VG)
C     NP - NUMBER OF WIND STATIONS
C     NSX - STARTING VALUE FOR X
C     NFX - END VALUE FOR X
C     NSY - STARTING VALUE FOR Y
C     NFY - END VALUE FOR Y
C     ITLE - TITLE OF PLOT
C     DIR - DIRECTION OF WIND AT STATION
C     SPD - VELOCITY OF WIND AT STATION
C     COR(I) - CORRECTION  (WHOLE DEGREES) AT STATION (I)
C     NAMST - NAMES OF THE STATIONS
C     CONFAC - CONVERSION FACTOR TO CHANGE WIND SPEED TO THE 100 FT LEVE
C
      DIMENSION DIR(50), SPD(50), U(50), V(50), X(50), Y(50), UG(13,16),
     1VG(13,16), ITLE(16),R3(10,13,16),N3(10,13,16),RT(30),NS8(30)
      DIMENSION D(31),   S(31),   LFLAG(25),COR(25)    ,NSV(13,16)
     1,CONFAC(25),NAMST(22)
      DIMENSION ISKIP(31),I1(3),I2(3),IRRAY1   (31),IRRAY2   (31),
     1          KMON(12)
      INTEGER*2 IWD(24,31)
      DATA I1,I2/2,3,5,2,4,11/
C     RTE - ROTATION OF NRTS ON GRID
C     RCH - RADIUS OF CIRCLE ENCLOSING DATA VALUES FOR INTERPOLATION
C     DX - SPACING OF GRID POINTS IN X-DIRECTION
C     DY - SPACING OF GRID POINTS IN Y-DIRECTION
C     DT - INCREMENTS OF TIME IN HOURS
C     DS - LENGTH OF SHAFT ON WIND ARROW
C     H - GRID INTERVAL IN MILES
C     X - X COORDINATE OF STATION
C     Y - YCCORDINATE OF STATION
      IF (KJ.EQ.1) GO TO 800
      IF (KN.NE.0) GO TO 1313
      KNR=0
  200 FORMAT(16A4)
      READ 11, NP, NSX, NSY, NFX, NFY,NSTL,INPT,NSKIP,KIST
   11 FORMAT (16I5)
      READ 12, RTE, RCH
   12 FORMAT (8F10.0)
      READ 10, (X(I), I=1,NP)
   10 FORMAT (16F5.0)
      READ 10, (Y(I), I=1,NP)
      READ 10, (COR(I),I=1,NP)
      RCH=RCH**2
      READ 40,(CONFAC(I), I=1,NP)
   40 FORMAT (16F5.2)
      CF1=CONFAC(1)
      CF2=CONFAC(2)
      CF4=CONFAC(4)
      READ 45,(NAMST(I),I=1,NP)
   45 FORMAT (16(1XA4))
      READ 71,   (ISKIP(I),I=1,31)
```

```
   71 FORMAT (3112)
      READ 200,(KMON(I),I=1,12)
      READ 42,YEAR
   42 FORMAT (A4,I6)
      PRINT 6666,(NAMST(I),I=1,NP)
 6666 FORMAT (1H1 4X22(1XA4))
      PRINT 630,(X(I),I=1,NP)
  630 FORMAT ('0 X =',22F5.1)
      PRINT 635,(Y(I),I=1,NP)
  635 FORMAT ('0 Y =',22F5.1)
      PRINT 44,(CONFAC(I),I=1,NP)
   44 FORMAT ('CCF =',22F5.2)
   19 FORMAT (1H1,16A4)
      KMAP=0
      KN=1
C*****SECTION FOR SETTING UP STATION ARRAY FOR EACH GRID POINT
      XG=NSX-1
      DO 730 I=NSX,NFX
      YG=NSY-1
      DO 720 J=NSY,NFY
      DO 705 L=1,NP
      NSB(L)=L
  705 RT(L)=(X(L)-XG)**2+(Y(L)-YG)**2
      CALL ASCND(RT,NSB,NP)
      DO 706 L=1,10
      R3(L,I,J)=RT(L)
  706 N3(L,I,J)=NSB(L)
  720 YG=YG+1.
  730 XG=XG+1.
      NPP=NP+1
      P18=3.1415927/180.
      IS=1
      READ 11,         MS,IDS,IHS
      KDS=IHS
      IF (NSKIP.EQ.0) GO TO 800
      DO 733 JLM=1,NSKIP
      IF (INPT.EQ.1) GO TO 731
      READ(8,END=732) IWD
      GO TO 733
  731 CALL BUFIN(8,IWD,186,NTATE,ICNT)
      CALL BUFDLY(8,0,0,NTATE,ICNT)
      IF (NTATE.NE.3) GO TO 733
  732 PRINT 734, IWD(24,1)
  734 FORMAT('0  END OF FILE READ FROM INPUT UNIT IN SKIP LOOP', I6)
      STOP
  733 CONTINUE
  800 NTATE=0
      ICNT=0
      IF (INPT.EQ.1) GO TO 735
      READ(8,END=736) IWD
      GO TO 5
```

```
  735 CALL BUFIN(8,IWD,186,NTATE,ICNT)
      CALL BUFDLY(8,0,0,NTATE,ICNT)
      IF (NTATE.NE.3) GO TO 5
  736 CONTINUE
      PRINT 50,IWD(24,1)
   50 FORMAT(' END OF.FILE REAC ON THE INPUT UNIT',10X,I5)
      STOP
    5 MON=IWD(1,1)/100
      IDAY=IWD(1,1)-MON*100
      IF(KNR.EQ.1) GO TO 1312
      IF (MON.NE.MS) GO TO 800
      IF (IDAY.NE.IDS) GO TO 800
      PRINT 1600,IHS,MON,IDAY,YEAR
 1600 FORMAT ('0 STARTING TIME = ',I2,':00',I3,'/',I2,'/',A3)
 1312 KJ=0
      KNR=1
      III=KDS-1
 1313 III=III+1
      IF(III.EQ.1) PRINT 1610,III,MON,IDAY,YEAR
 1610 FORMAT (' ' 95X 'NEW RECORD  ',I2,':00',I3,'/',I2,'/',A3)
      IF(IWD(III,1).NE.0) GO TO 1615
      III=III-1
      GO TO 896
 1615 M=0
      DO 210 J=1,31
      IRRAY1  (J)=0.
      IRRAY2  (J)=0.
      IF (ISKIP (J).EQ.0) GO TO 210
      M=M+1
      IRRAY1(M)=IWD(III,J)/100
      IRRAY2(M)=IWD(III,J)-IRRAY1(M)*100
  210 CONTINUE
      PRINT 9300,(IRRAY1(J),IRRAY2(J),J=1,M)
 9300 FORMAT(1H0,5X,25(2I2,1X))
  300 CONTINUE
      DO 60 J=1,M
      D(  J)=IRRAY1(  J)
   60 S(  J)=IRRAY2(  J)
C*****END STATION ARRAY SECTION
      JI=0
      MHR=III*100
      JJ=D(1)+.1
      JK=S(1)+.1
 1501 DO 1317 IN=2,NPP
      JI=JI+1
      DIN=D(IN)
      SII=S(IN)
      IF (DIN - 89.       ) 1315,1314,1314
 1314 LFLAG(JI)=1
      U(JI)=0.0
      V(JI)=0.0
```

```
      GO TO 1317
 1315 IF (SII - 89.     ) 1316,1314,1314
 1316 LFLAG(JI)=0
      IF (DIN.LE.36) GO TO 1320
      LFLAG (JI)=2
      DIN=DIN-50.
 1320 DIR(JI)=      DIN *10. +CCR(JI)
      SPD(JI)=      SII *CONFAC(JI)
 1317 CONTINUE
 1319 KSR=0
      DO 15 I=1,NP
      IF (LFLAG(I)-1) 1318,15,1318
 1318 CR=DIR(I)-RTE
      ANG=(270-DR)*P18
      U(I)=SPD(I)*COS(ANG)
      V(I)=SPD(I)*SIN(ANG)
   15 CONTINUE
      IF(K1ST.GT.0) GO TO 900
C*****INTERPOLATION SECTION BEGIN
   49 DO 895 I=NSX,NFX
      DO 890 J=NSY,NFY
      SNU=0.0
      SNV=0.0
      SND=0.0
      NS=0
      DO 870 L=1,10
      LS = N3(L,I,J)
      RS = R3(L,I,J)
      IF (LFLAG(LS).EQ.1) GO TO 870
      IF (RS.LE.1.E-15) GO TO 850
      IF (NS.LT.NSTL) GO TO 820
      IF (RS.GT.RCH) GO TO 875
  820 RSI=1./RS
      SNU=SNU+U(LS)*RSI
      SNV=SNV+V(LS)*RSI
      SND=SND+RSI
      NS=NS+1
      GO TO 870
  850 UG(I,J)=U(LS)
      VG(I,J)=V(LS)
      NSV(I,J)=1
      GO TO 890
  870 CONTINUE
  875 UG(I,J)=SNU/SND
      VG(I,J)=SNV/SND
  890 CONTINUE
  895 CONTINUE
      NSV(I,J)=NS
      PRINT 9500,(U(J),J=1,NP)
      PRINT 9500,(V(J),J=1,NP)
 9500 FORMAT(11X,23F5.1)
```

```
      GO TO 950
  900 IF(LFLAG(K1ST).NE.1) GO TO 920
      PRINT 910,NAMST(K1ST),III,IDAY,MON,YEAR,U(K1ST),V(K1ST)
  910 FORMAT (1HO,A4,' MISSING AT ',I4,':00 ',I4,'/',I2,'/',A3,' SINGLE STATI
     1ON ANALYSIS CONTINUING WITH U,V= ',2F6.2)
  920 DO 930 I=NSX,NFX
      DO 930 J=NSY,NFY
      UG(I,J)=U(K1ST)
  930 VG(I,J)=V(K1ST)
  950 CONFAC(1)=CF1
      CONFAC(2)=CF2
      CONFAC(4)=CF4
      KMAP=KMAP+1
  825 IF (III.LT.24) GO TO 896
      KDS=1
      KJ=1
  896 RETURN
      END
```

```
      SUBROUTINE ASCND (X,N,NP)
      DIMENSION X(20),N(20)
      NP1=NP-1
      DO 50 I=1,NP1
      KI=0
      DO 40 K=1,NP1
      IF(X(K+1).GT.X(K)) GO TO 40
      KI=K+1
      TMP=X(K)
      NTMP=N(K)
      X(K)=X(KI)
      N(K)=N(KI)
      X(KI)=TMP
      N(KI)=NTMP
   40 CONTINUE
      IF (KI.EQ.0) GO TO 60
   50 CONTINUE
   60 CONTINUE
      RETURN
      END
```


☆U.S. GOVERNMENT PRINTING OFFICE 1974 - 677-232/1210 REG. 8